Extensions of Perturbation Theory for Spin Dressed Neutrons and 3He Comagnetometers in Superfluid 4He

Adam Lipman *

Posted Date: 5 September 2024

doi: 10.20944/preprints202409.0474.v1

Keywords: spin dressing; ultra cold neutrons; magnetic resonance; quantum mechanics; perturbation theory

Article

Extensions of Perturbation Theory for Spin Dressed Neutrons and 3He Comagnetometers in Superfluid ^{4}He

Adam Lipman

North Carolina State University; adamlipman13@gmail.com

Abstract: The nEDM experiment at Oak Ridge's Spallation Neutron Source will probe for an electric dipole moment of the neutron at an unprecedented level of sensitivity. Polarized 3He atoms dressed by a radio-frequency field are a crucial component. For field parameters comparable to the parameters being used in the nEDM experiment, numerical studies using a fourth-order Runge-Kutta solver reveal inadequacies in earlier analyses of 3He spin dynamics. It's seen that neutron absorption is influenced by avoided level-crossings omitted previously. Also, the critical dressing condition, used to eliminate effects of the static magnetic field, requires modification. First-order perturbative corrections to eigenstates and third-order corrections to eigenenergies are needed to account for the impact of avoided level-crossings and the changes in the critical dressing condition, respectively.

Keywords: spin dressing; ultra cold neutrons; magnetic resonance; quantum mechanics; perturbation theory

1. Spin Dressing Theory

1.1. Spin Dressing Introduction

Understanding the dynamics of spin dressing in regards to the nEDM experiment is crucial for reliable measurements at never before reached sensitives. From the Golub, Lamoreaux Physics Reports paper [1], the Hamiltonian in Equation 1 contains everything I need for a basic spin dressing framework. Given a spin 1/2 particle in a static magnetic field B_0 along +z and an oscillating magnetic field along x with frequency ω, the quantized Hamiltonian is

$$H = \omega a^* a + \gamma\sqrt{2\pi\hbar\omega/L^3}s_x(a + a^*) + \omega_0 s_z, \tag{1}$$

where γ is the gyromagnetic ratio of the particle, $\omega_0 = -\gamma B_0$ and L^3 is the volume of the trap. I will treat the last term in Equation 1, the static field term, as a perturbation. The Hamiltonian can be transformed [2] such that the unperturbed eigenstates can be defined as

$$\begin{aligned}\overline{|n, m_x\rangle} &= e^{-(\lambda s_x/\omega)(a^*-a)}|n\rangle|m_x\rangle \\ &= e^{-(\lambda m_x/\omega)(a^*-a)}|n\rangle|m_x\rangle = \overline{|n_{m_x}\rangle}|m_x\rangle,\end{aligned} \tag{2}$$

where $|m_x\rangle$ is an eigenstate of s_x with eigenvalue m_x and for a spin 1/2 particle, $m_x = \pm 1/2$. Going forward, I will express $|m_x\rangle$ states at $|+\rangle_x$ or $|-\rangle_x$. $|n\rangle$ is an eigenstate of a^*a with eigenvalue n. $\lambda = \gamma\sqrt{2\pi\hbar\omega/L^3}$ and its definition starts from the energy density of magnetic field B_1 given as $B_1^2/2 = 4\pi n_{av}\hbar\omega/L^3 = 2n_{av}\lambda^2/\gamma^2$ such that $\omega_1^2 = 4n_{av}\lambda^2$ where $\omega_1 = \gamma B_1$.

After the transformation, the energy eigenvalues, which are the degenerate in m_x, present themselves as

$$E_{n,m_x} = n\omega - \frac{m_x^2\lambda^2}{\omega}. \tag{3}$$

With the Hamiltonian now transformed, expectation values will require calculation of the inner product of two bar states. The calculation and proof originally done in [2] is shown in Appendix A. The Physics Reports [1] has the m_z eigenstates as

$$\overline{|n, m\rangle}_z = \frac{1}{\sqrt{2}}(\overline{|n_+\rangle}|+\rangle_x + im\overline{|n_-\rangle}|-\rangle_x) \tag{4}$$

 doi:10.20944/preprints202409.0474.v1

where $m = 2m_z$ and is an equivalent form of the eigenvectors shown in Appendix A for spin along +z and -z ($m = \pm 1$). Going forward, I will write m_z as m and any spin states with a + or - is a state in the x basis.

1.2. Expectation Values

Given Equation 4 are eigenstates that lift the degeneracy in the Hamiltonian, I can now derive expressions for spin expectation values as done in [1]. For each component that follows, I will first show the matrix elements using Equation 4 and then incorporate the elements into a time dependent wave function.

The matrix elements for σ_y are

$$\begin{aligned}
&\overline{\langle n', m'|}\sigma_y\overline{|n, m\rangle} \\
&= \frac{1}{2}\Big(\overline{\langle n'_+|}\langle +| - im'\overline{\langle n'_-|}\langle -|\Big)(|+\rangle\langle -| + |-\rangle\langle +|) \\
&\quad \times \Big(\overline{|n_+\rangle}|+\rangle + im\overline{|n_-\rangle}|-\rangle\Big) \\
&= \frac{1}{2}\Big(im\overline{\langle n'_+|n_-\rangle} - im'\overline{\langle n'_-|n_+\rangle}\Big) \\
&= \frac{1}{2}\Big(m\overline{\langle (n-q)_+||n_-\rangle} - m'\overline{\langle (n-q)_-||n_+\rangle}\Big) \\
&= \frac{1}{2}i\Big(mJ_{-q}(\omega_1/\omega) - m'J_q(\omega_1/\omega)\Big) \\
&= \frac{1}{2}i\Big(mJ_q(\omega_1/\omega)(-1)^q - m'J_q(\omega_1/\omega)\Big),
\end{aligned} \tag{5}$$

so that the expectation value is

$$\begin{aligned}
&< \sigma_y(t) >= \sum_{m',q}\sum_{n,n'}\frac{1}{2}a^*_{n'}a_n e^{-in'\omega t}e^{-im'\omega_d t/2}i \\
&\times\Big(mJ_q(\omega_1/\omega)(-1)^q - m'J_q(\omega_1/\omega)\Big)e^{im\omega_d t/2}e^{in\omega t}.
\end{aligned} \tag{6}$$

a_n are Glauber coefficients which describe the probability amplitudes of photons of a harmonic field. They can be expressed as

$$a_n = e^{-\lambda/2}\frac{\lambda^{n/2}}{(n!)^{1/2}}, \tag{7}$$

where $\lambda =< n >$, the average photon number. Then for large n, $\sum_n |a_n|^2 = 1$. Given selection rules on m and m' and summing over these values, the expectation value for σ_y becomes

$$\begin{aligned}
&< \sigma_y(t) >= \sum_{m',q}\frac{1}{2}e^{iq\omega t}e^{-i/2(m'-m)\omega_d t}i \\
&\times\Big(mJ_q(\omega_1/\omega)(-1)^q - m'J_q(\omega_1/\omega)\Big) \\
&= -J_0(\omega_1/\omega)\sin\omega_d t \\
&- \sum_{q>0,even}J_q(\omega_1/\omega)\big[\sin(\omega_d + q\omega)t + \sin(\omega_d - q\omega)t\big].
\end{aligned} \tag{8}$$

 doi:10.20944/preprints202409.0474.v1

For σ_z, the matrix elements are

$$\begin{aligned}
&\overline{\langle n', m'|}\sigma_z\overline{|n, m\rangle} \\
&= \frac{1}{2}\Big(\overline{\langle n'_+|}\langle +| - im'\overline{\langle n'_-|}\langle -|\Big)(-i|+\rangle\langle -| + i|-\rangle\langle +|) \\
&\quad \times \Big(\overline{|n_+\rangle}|+\rangle + im\overline{|n_-\rangle}|-\rangle\Big) \\
&= \frac{1}{2}\Big(mJ_{-q}(\omega_1/\omega) + m'J_q(\omega_1/\omega)\Big) \\
&= \frac{1}{2}\Big(mJ_q(\omega_1/\omega)(-1)^q + m'J_q(\omega_1/\omega)\Big).
\end{aligned} \tag{9}$$

So that the expectation value is

$$\begin{aligned}
< \sigma_z(t) > &= \sum_{m',q}\sum_{n,n'}\frac{1}{2}a^*_{n'}a_n e^{-i(n'-n)\omega t}e^{-i/2(m'-m)\omega_d t} \\
&\quad \times \Big[mJ_q(\omega_1/\omega)(-1)^q + m'J_q(\omega_1/\omega)\Big] \\
&= \sum_{q>0,odd} J_q(\omega_1/\omega)\big[\cos(\omega_d - q\omega)t - \cos(\omega_d + q\omega)t\big].
\end{aligned} \tag{10}$$

And finally, for σ_x

$$\begin{aligned}
&\overline{\langle n', m'|}\sigma_x\overline{|n, m\rangle} \\
&= \frac{1}{2}\Big(\overline{\langle n'_+|}\langle +| - im'\overline{\langle n'_-|}\langle -|\Big)(|+\rangle\langle +| - |-\rangle\langle -|) \\
&\quad \Big(\overline{|n_+\rangle}|+\rangle + im\overline{|n_-\rangle}|-\rangle\Big) \\
&= \frac{1}{2}\delta_{n,n'}(1 - m'm).
\end{aligned} \tag{11}$$

So that the expectation value is

$$\begin{aligned}
< \sigma_x(t) > &= \sum_{m,q}\sum_{n,n'}\frac{1}{2}a^*_{n'}a_n e^{-in'\omega t}e^{-im'\omega_d t/2} \\
&\quad \times \delta_{n,n'}(1 - m'm)e^{in\omega t}e^{i'\omega_d t/2} \\
&= \sum_{n,m,m'}\frac{1}{2}a^*_n a_n e^{-i/2(m'-m)\omega_d t}(1 - m'm) = \cos\omega_d t.
\end{aligned} \tag{12}$$

Thus, I have expressions for how spin expectations values evolve through time.

When it comes to my simulation work, the comparison of simulation data versus these expressions is important to benchmark the simulations before extending them to higher complexities. After making a fourth order Runge-Kutta (RK4) solver in Matlab to solve the spin Bloch equations, I saw there were frequencies matching with theory as well as additional frequencies which have not been accounted for in the Physics Reports. Furthermore, I saw confluence of the RK4 results with the near-exact Hamiltonian method shown in a later section. Given how the RK4 results vary with the parameter $y = \omega_0/\omega$, perturbation theory became my focus to try to account for the additional frequencies. Also, the experiment uses $y = 0.10$ and so examination of whether this parameter is sufficiently small to only use the first order corrections to the eigenvalues is quite important.

2. The 4th Order Runge-Kutta Solver for the Spin Bloch Equations

The spin Bloch equations can be solved in Matlab by constructing a fourth-order Runge-Kutta solver. Given the Bloch equations

 doi:10.20944/preprints202409.0474.v1

$$\frac{d\vec{S}}{dt} = \gamma(\vec{S} \times \vec{B}), \tag{13}$$

I can specify field parameters, time steps, simulation time and initial conditions as inputs into my RK4. For spin dressing, I simply have to use the appropriate fields and solve for the spin components. The fields will be

$$\begin{gathered} \vec{B_x}(t) = B_1 \cos\omega t\hat{i} \\ B_y = 0 \\ \vec{B_z} = B_0\hat{k} \\ y \equiv \omega_0/\omega, \quad x \equiv \gamma_n B_1/\omega = \omega_1/\omega. \end{gathered} \tag{14}$$

An example of a three dimensional spin dressing simulation between UCN and ^{3}He is shown in Figure 1.

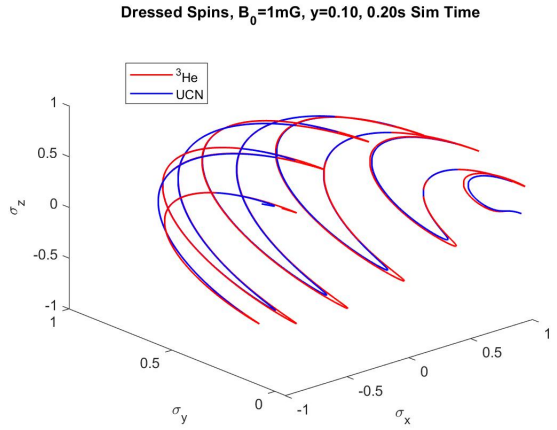

Figure 1. ^{3}He in red and UCN in blue, the two critically dressed for 0.20s of simulation time.

Using initial conditions on the time dependent spin components $S_i(t)$ of $S_x(0) = 1$, $S_y(0) = 0$ and $S_z(0) = 0$, time steps of tstep $= 0.0005$ seconds for the spin components and tstep$/2$ for magnetic field time steps, the RK4 will solve for each spin time series.

For the rest of this chapter, the simulation time is $T = 10.0s$ (the actual computation can take anywhere from minutes to hours). For the number of particles, I will use $N = 1$. Finally, the first results I will show have field parameters of

$$\begin{gathered} B_0 = 1\text{mG} \\ y = 0.10, x = 1.189. \end{gathered} \tag{15}$$

The results are spins as a function of time: $\sigma_x(t)$, $\sigma_y(t)$ and $\sigma_z(t)$. I then take the fast Fourier transform (FFT) of these time series and to see relevant frequencies. From the theory in the previous section, I expect certain frequencies for each spin component. The plots in Figures 2 to 4 are the FFTs of the spins for the parameters in Equation 15. In light green is simulation data and in black is theory using the expectation values from last section. The time steps are very small and therefore the frequency range is large so the plots are zoomed in for better inspection of the relevant frequencies.

Preprints.org (www.preprints.org) | NOT PEER-REVIEWED | Posted: 5 September 2024 doi:10.20944/preprints202409.0474.v1

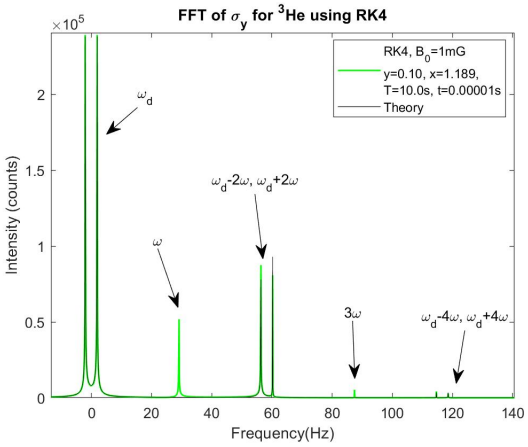

Figure 2. σ_y for $y = 0.10$, frequencies solved for using the RK4 method. ω and 3ω are frequencies not currently included in theory.

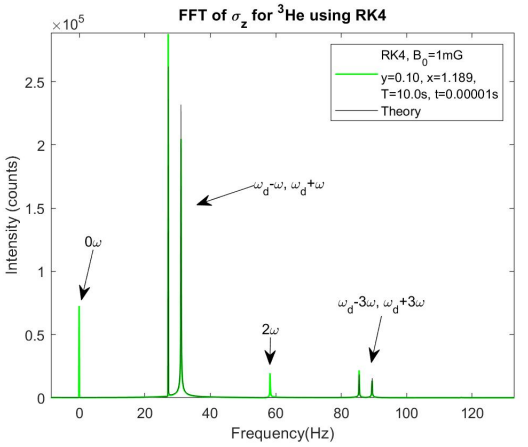

Figure 3. σ_z for $y = 0.10$, frequencies solved for using the RK4 method. 0ω and 2ω are frequencies not currently included in theory.

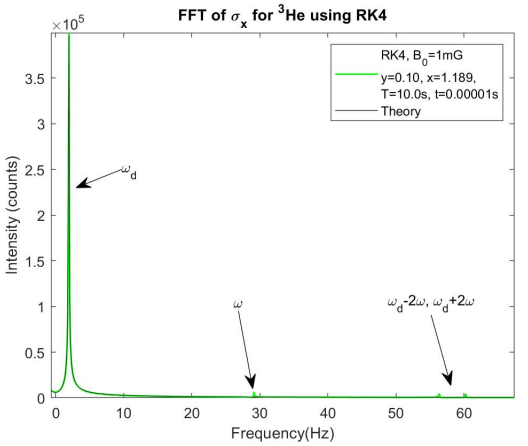

Figure 4. σ_x for $y = 0.10$, frequencies solved for using the RK4 method. ω and $\omega_d \pm 2\omega$ are frequencies not currently included in theory.

The theory in Figures 2-4 are the predicted results from Equations 8, 10 and 12, respectively. As seen, there are frequencies and harmonics consistent with the expectation values in that section. Furthermore, the ratio of the heights of the expected peaks are in-line with ratios of amplitudes of

 doi:10.20944/preprints202409.0474.v1

Bessel functions of the first kind of corresponding order. But what is quite interesting are the peaks that the theory doesn't predict. In Figure 4 for σ_x, I see these 'unexpected' frequencies of ω and $\omega_d \pm 2\omega$ are almost negligible. But in Figure 2 showing σ_y, the unexpected peaks at ω and 3ω are not negligible. And for σ_z in Figure 3, the unexpected frequencies of 0ω and 2ω have meaningful intensities as well. Figures 5 and 6 show what Figures 3 and 4 showed but for $y = 0.01$ meaning ω is ten times larger.

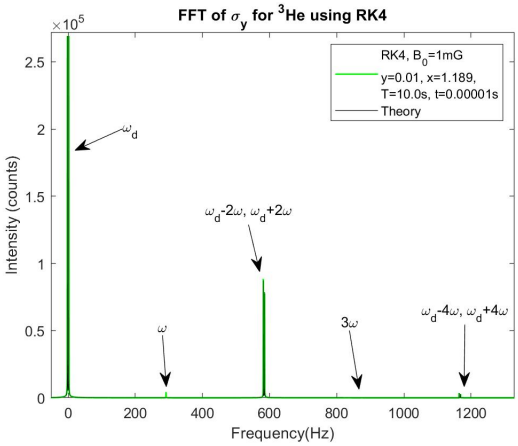

Figure 5. σ_y for $y = 0.01$, frequencies solved for using the RK4 method. ω and 3ω are frequencies not currently included in theory.

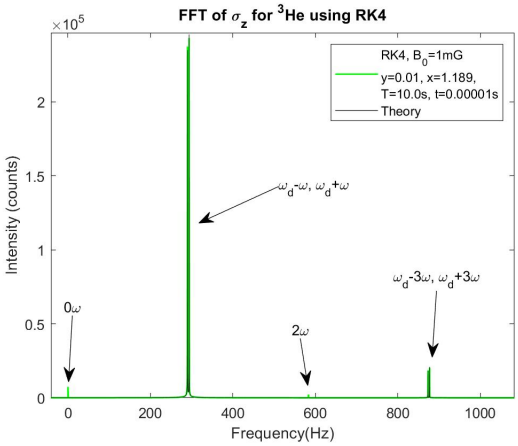

Figure 6. σ_z for $y = 0.01$, frequencies solved for using the RK4 method. 0ω and 2ω are frequencies not currently included in theory.

What's interesting is that the unexpected frequencies decreased in height substantially between $y = 0.10$ and $y = 0.01$. Given y is a measure of the perturbing static field relative to the rate of oscillation of the dressing field, intensity dependence on y points to missing higher order perturbation theory terms.

The question then is: are these unexpected frequencies due to the RK4 numerical solver issues in Matlab or is it from higher order perturbation theory terms? The reduction in intensity when y is smaller would suggest the latter. Some theoretical models use y anywhere between 0.10 and 0.01 while the experiment will use $y = 0.10$. Figures 7 to 9 show how these unexpected frequency peaks change as the perturbation strength changes. I chose two frequencies from σ_x (ω and $\omega_d - 2\omega$) and one each from σ_y (ω) and σ_z (0ω). Then stepped y by 0.0001 between 0.01 and 0.10.

 doi:10.20944/preprints202409.0474.v1

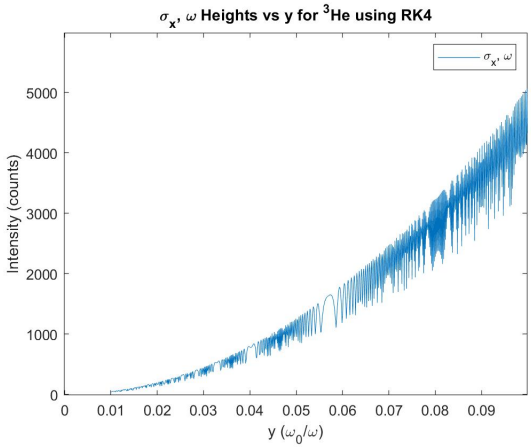

Figure 7. $\sigma_x\ \omega$ heights vs y using the RK4. Intensity ranges from 36 to 4031

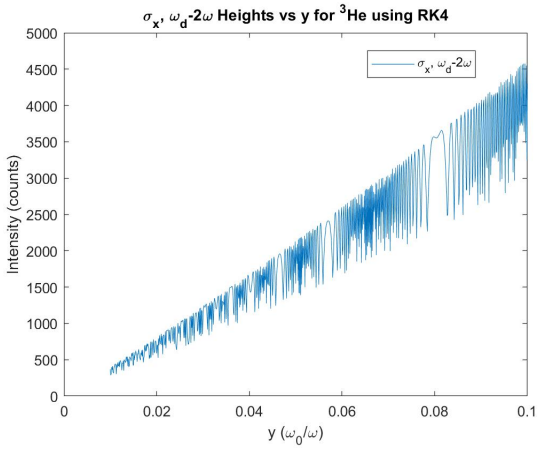

Figure 8. $\sigma_x\ \omega_d - 2\omega$ heights vs y using the RK4. Intensity ranges from 370 to 4304.

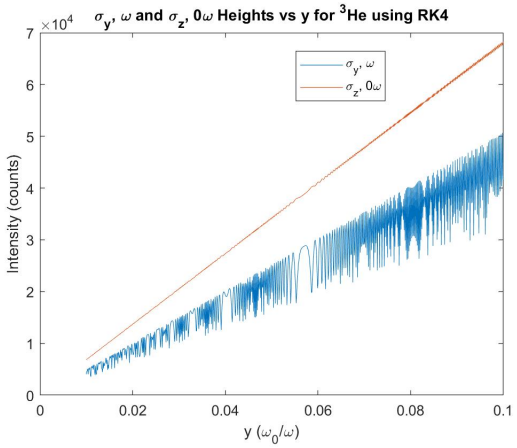

Figure 9. $\sigma_y\ \omega$ and $\sigma_z\ 0\omega$ heights vs y using the RK4. Intensity ranges from 4050 to 41863 and 6861 to 68212 respectively.

The oscillatory behavior in Figures 7 to 9 most likely comes from numerical issues within the solver. From Figure 9, the unexpected frequencies I chose from σ_y and σ_z show linear in y dependence. And from Figures 7 and 8, unexpected frequencies for σ_x show y^2 and y dependence respectively. Going forward, I will call these unexpected frequencies ***anomalies***.

 doi:10.20944/preprints202409.0474.v1

Given the dependence on y, the anomalies most likely come from perturbation theory. The next section shows a different method for solving for expectation values and frequencies of spin components to provide further evidence that the anomalies are not artifacts. If it can give confluence to the RK4 method, I will use higher order perturbation theory to more accurately represent this system.

3. The Hamiltonian Method

3.1. Theory

Diagonalizing the Hamiltonian in Equation 1 is a method that for high photon number N_p, converges towards an exact solution. However, computation time is a limiting factor. For N_p very large, n_{av} refers to an addition or subtraction away from N_p. This also means the $\sqrt{n_{av}}$ in λ can be ignored. I will write n_{av} as n going forward. Given this Hamiltonian and how the creation and annihilation operators effect adjacent states, the Hamiltonian matrix in the z basis up to $n = \pm 2$ can be written as

$$\begin{pmatrix} 2+a & 0 & 0 & b & 0 & 0 & 0 & 0 & 0 & 0 \\ 0 & 2-a & b & 0 & 0 & 0 & 0 & 0 & 0 & 0 \\ 0 & b & 1+a & 0 & 0 & b & 0 & 0 & 0 & 0 \\ b & 0 & 0 & 1-a & b & 0 & 0 & 0 & 0 & 0 \\ 0 & 0 & 0 & b & 0+a & 0 & 0 & b & 0 & 0 \\ 0 & 0 & b & 0 & 0 & 0-a & b & 0 & 0 & 0 \\ 0 & 0 & 0 & 0 & 0 & b & -1+a & 0 & 0 & b \\ 0 & 0 & 0 & 0 & b & 0 & 0 & -1-a & b & 0 \\ 0 & 0 & 0 & 0 & 0 & 0 & 0 & b & -2+a & 0 \\ 0 & 0 & 0 & 0 & 0 & 0 & b & 0 & 0 & -2-a \end{pmatrix}_z \tag{16}$$

where $a = y/2$ and $b = x/4$. Additionally, I can write the Hamiltonian matrix in the x or nbar basis but for my simulations, I used the z basis.

3.2. Solving for Eigenvalues, Eigenvectors and Time Evolution Operators

Solving for the eigenvalues and eigenvectors will be the large majority of the computation. For calculating the expectation values of time dependent spin components, initialization of the state and spin matrices are needed. Specifically, in the z basis and an initial state ψ_0 along +x, ψ_0 will take the form of an Nx1 column vector of all ones and a normalization factor. The spin component operators will be NxN matrices with 2x2 Pauli matrices along their respective diagonals.

With the eigenvalues known, I move to calculating time evolution operators

$$U_i = e^{-iwt_i\lambda}, \tag{17}$$

where t_i is just an element in the array t representing time and since I will use $T = 10.0s$ and tstep= 0.0005s, t is a 1x20001 array. λ is the diagonal eigenvalues matrix so that U is an NxN diagonal matrix at a given time.

$\psi(t)$ is constructed by transforming U into the eigenvector basis, letting it evolve, then transforming back and multiplying it onto ψ_0

$$\psi_i(t) = K^+ U_i(t) K \cdot \psi_0, \tag{18}$$

where K is the NxN eigenvector matrix. Finally, the expectation values over time take the usual form of

$$S_i(t) = \psi(t)^+ S_i \psi(t). \tag{19}$$

The results are spin components as time arrays just like in the RK4 and I proceed to take fast Fourier transforms of them to extract frequencies. What I saw was agreement between this method and the RK4. At first, for low N, the Hamiltonian method was all over the place. But as N got larger, the results converged towards what the RK4 showed.

 doi:10.20944/preprints202409.0474.v1

3.3. Comparing the Hamiltonian Method to the RK4

The Hamiltonian method showed reasonable results for $n = \pm 150$ which is $N = 602$. However, to be more accurate, I will use $n = \pm 200$ in the following plots. Figures 10 to 13 show σ_y and σ_z for $y = 0.10$ and $y = 0.01$ and as with the RK4 plots, I have zoomed in to show relevant frequencies.

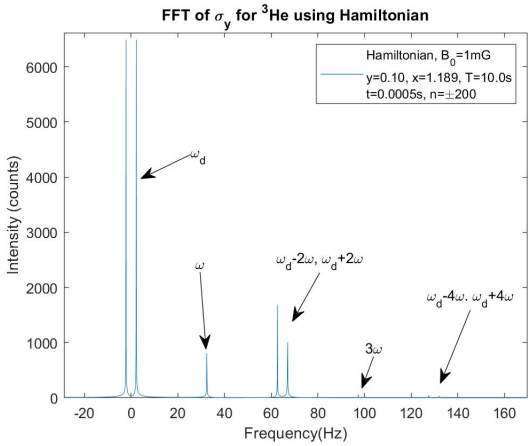

Figure 10. σ_y frequencies for y=0.10 using the Hamiltonian method, N=802.

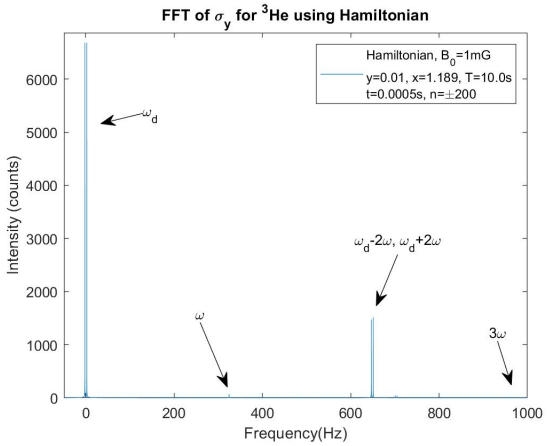

Figure 11. σ_y frequencies for y=0.01 using the Hamiltonian method, N=802.

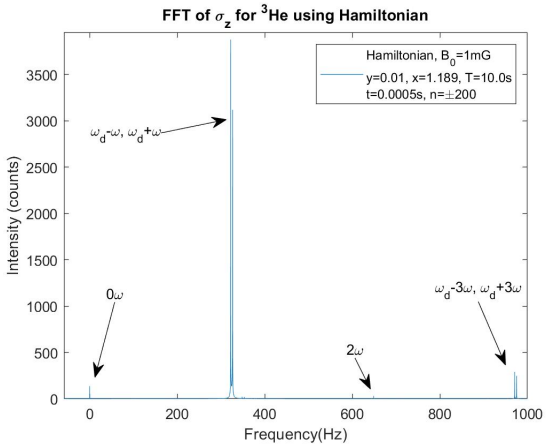

Figure 12. σ_z frequencies for y=0.10 using the Hamiltonian method, N=802.

 doi:10.20944/preprints202409.0474.v1

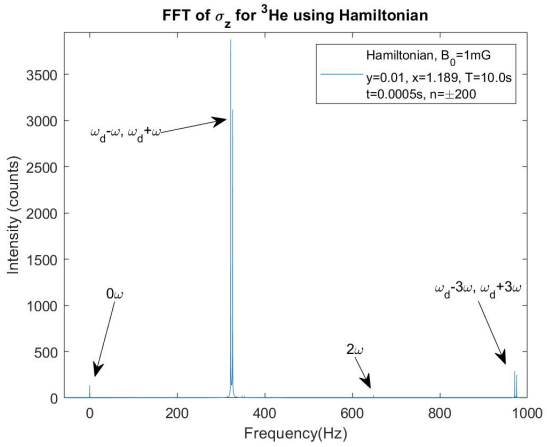

Figure 13. σ_z frequencies for y=0.01 using the Hamiltonian method, N=802.

The immediate conclusion is that the Hamiltonian method is showing very similar results to the RK4 method. The difference in heights between the two methods mostly comes from the difference in time stepping and therefore total intensity. The ratio of heights between the two methods as well as the ratio of heights within a method and compared to the other would converge for n much larger. And again, I am seeing the anomalous frequency heights decreasing as y gets smaller. For comparison to Figure 9, I will loop through four values of y: 0.10, 0.05, 0.02 and 0.01 and show the results for $n = \pm 200$ in Figure 14. The reason I'm only using four values whereas the RK4 plots used 901 y values is because each Hamiltonian method simulation takes a long time. The plot shows a near linear relationship for these anomalies' heights and y, as seen before.

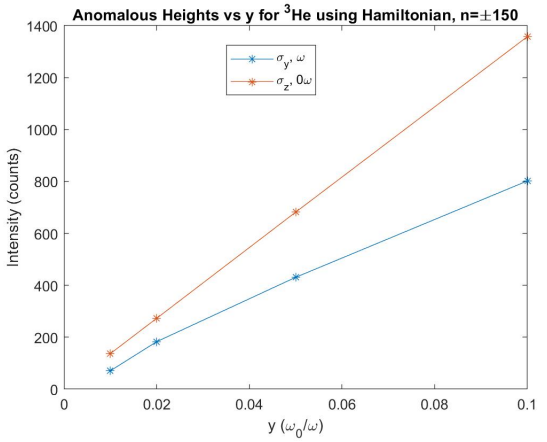

Figure 14. σ_y and σ_z y vs. frequency peaks, solved using the Hamiltonian method for $n = \pm 150$.

4. First Order Perturbation Theory, Corrections to the Eigenstates

In the first section, the degeneracy was lifted by finding first order energy shifts. The m_z eigenvectors were then used for calculating expectation values. Given the evidence laid out in the sections showing results from the RK4 and Hamiltonian methods, it's clear extensions of perturbation theory are needed to account for the anomalous frequencies. More specifically, corrections to the eigenstates are required rather than corrections to the eigenvalues. This is because the only way for the peak heights to have a dependence on y^n, where n is the order of perturbation theory, is from corrections to the eigenstates. Whereas corrections to the eigenvalues introduce changes to energy levels and therefore frequencies.

An expansion of an eigenstate using higher order corrections is written as

$$\overline{|n,m\rangle} = \overline{|n,m\rangle}^{(0)} + \overline{|n,m\rangle}^{(1)} + ... \tag{20}$$

 doi:10.20944/preprints202409.0474.v1

The first term on the right hand side are the m_z eigenstates whereas the second term is the 1st order correction.

$$\overline{|n,m\rangle}^{(0)} = \frac{1}{\sqrt{2}}\left[\overline{|n_+\rangle}|+\rangle + im\overline{|n_-\rangle}|-\rangle\right]. \tag{21}$$

The first order correction is generally written as

$$\left|n^{(1)}\right\rangle = \sum_{k\neq n} \frac{\left\langle k^{(0)}\middle|V\middle|n^{(0)}\right\rangle}{E_n^{(0)} - E_k^{(0)}}\left|k^{(0)}\right\rangle, \tag{22}$$

and so first order corrections to unprimed and primed states are

$$\begin{aligned}\overline{|n,m\rangle}^{(1)} &= \sum_{n'',m''} \frac{\overline{\langle n'',m''|}\frac{1}{2}\omega_0\sigma_z\overline{|n,m\rangle}}{E_n^0 - E_{n''}^0}\overline{|n'',m''\rangle} \\ &= \sum_{m''}\sum_{q'\neq 0} \frac{\frac{1}{4}\omega_0\left[mJ_{q'}(x)(-1)^{q'} + m''J_{q'}(x)\right]}{(n-n'')\omega}\overline{|n'',m''\rangle} \\ &= y\sum_{m''}\sum_{q'\neq 0} A(m,m',q')\overline{|n'',m''\rangle},\end{aligned} \tag{23}$$

where I define A as

$$A(m,m',q') = \frac{\left[mJ_{q'}(x)(-1)^{q'} + m''J_{q'}(x)\right]}{4q'}. \tag{24}$$

For the primed states

$$\begin{aligned}\overline{|n',m'\rangle}^{(1)} &= \sum_{n'',m''} \frac{\overline{\langle n'',m''|}\frac{1}{2}\omega_0\sigma_z\overline{|n',m'\rangle}}{E_{n'}^0 - E_{n''}^0}\overline{|n'',m''\rangle} \\ &= \sum_{m''}\sum_{q'-q\neq 0} \frac{\frac{1}{4}\omega_0\left[m'J_{q'-q}(x)(-1)^{q'-q} + m''J_{q'-q}(x)\right]}{(n'-n'')\omega}\overline{|n'',m''\rangle} \\ &= y\sum_{m''}\sum_{q'\neq 0} A'(m,m',q,q')\overline{|n'',m''\rangle},\end{aligned} \tag{25}$$

where I define A' as

$$A'(m,m',q,q') = \frac{\left[m'J_{q'-q}(x)(-1)^{q'-q} + m''J_{q'-q}(x)\right]}{4(q'-q)}. \tag{26}$$

From before, $q = n - n'$ but now $q' = n - n''$ such that $n' - n'' = q' - q$. States cannot be equal in the formulation of the first order corrections which then requires $q' \neq 0$ and $q' - q \neq 0$ for certain values of m, m', m'' but also to avoid singularities.

Now a state $\overline{|n,m\rangle}$ up to first order is

$$\begin{aligned}\overline{|n,m\rangle} = \frac{1}{\sqrt{2}}\Bigg[&\overline{|n_+\rangle}|+\rangle + im\overline{|n_-\rangle}|-\rangle \\ &+y\sum_{n'',m''}\sum_{q'\neq 0} A(m,m',q')\left[\overline{|n''_+\rangle}|+\rangle + im''\overline{|n''_-\rangle}|-\rangle\right]\Bigg].\end{aligned} \tag{27}$$

Preprints.org (www.preprints.org) | NOT PEER-REVIEWED | Posted: 5 September 2024 doi:10.20944/preprints202409.0474.v1

And similarly, a state $\overline{|n',m'\rangle}$ up to first order is

$$\begin{aligned}\overline{|n',m'\rangle} &= \frac{1}{\sqrt{2}}\Big[\overline{|n'_+\rangle}|+\rangle + im'\overline{|n'_-\rangle}|-\rangle \\ &+y\sum_{n'',m''}\sum_{q,q'\neq 0}A'(m,m',q,q')\left[\overline{|n''_+\rangle}|+\rangle + im''\overline{|n''_-\rangle}|-\rangle\right]\Big].\end{aligned} \tag{28}$$

The matrix elements for σ_y are

$$\begin{aligned}\overline{\langle n',m'|}\sigma_y\overline{|n,m\rangle} &= \frac{1}{2}\Big[\left[\langle+|\overline{\langle n'_+|} - im'\langle-|\overline{\langle n'_-|}\right] \\ &+yA'^{*}(m,m',q,q')\left[\langle+|\overline{\langle n''_+|} - im''\langle-|\overline{\langle n''_-|}\right]\Big] \\ &\times\left[|+\rangle\langle-| + |-\rangle\langle+|\right]\times\Big[\left[\overline{|n_+\rangle}|+\rangle + im\overline{|n_-\rangle}|-\rangle\right] \\ &+yA(m,m',q')\left[\overline{|n''_+\rangle}|+\rangle + im''\overline{|n''_-\rangle}|-\rangle\right]\Big] \\ &= \frac{1}{2}\Big[\left[\langle+|\overline{\langle n'_+|} - im'\langle-|\overline{\langle n'_-|}\right] \\ &+yA'^{*}(m,m',q,q')\left[\langle+|\overline{\langle n''_+|} - im''\langle-|\overline{\langle n''_-|}\right]\Big] \\ &\times\Big[\left[\overline{|n_+\rangle}|-\rangle + im\overline{|n_-\rangle}|+\rangle\right] \\ &+yA(m,m',q')\left[\overline{|n''_+\rangle}|-\rangle + im''\overline{|n''_-\rangle}|+\rangle\right]\Big] \\ &= \frac{1}{2}\Big[im\overline{\langle n'_+|n_-\rangle} - im'\overline{\langle n'_-|n_+\rangle} \\ &+iyA'^{*}(m,m',q,q')\left[m\overline{\langle n''_+|n_-\rangle} - m''\overline{\langle n''_-|n_+\rangle}\right] \\ &+iyA(m,m',q')\left[m''\overline{\langle n'_+|n''_-\rangle} - m'\overline{\langle n'_-|n''_+\rangle}\right] + O(y^2)\Big],\end{aligned} \tag{29}$$

where the first two terms in the brackets are the usual zeroth order, unperturbed terms and $O(y^2)$ refers to terms proportional to y^2 that I will ignore. Then, the expectation value is

$$\begin{aligned}&<\sigma_y(t)> \\ &= \sum_{m,m',m''}\sum_{q,q'}\frac{1}{2}a^*_{n'}a_n e^{iq\omega t}e^{i(m-m')\omega_d t/2}\times\Big[imJ_q(x)(-1)^q - im'J_q(x) \\ &+iy\frac{\left[m'J_{q'-q}(x)(-1)^{q'-q} + m''J_{q'-q}(x)\right]}{4(q'-q)}\left[mJ_{q'}(x)(-1)^{q'} - m''J_{q'}(x)\right] \\ &+iy\frac{\left[mJ_{q'}(x)(-1)^{q'} + m''J_{q'}(x)\right]}{4q'}\left[-m'J_{q'-q}(x) + m''J_{q'-q}(x)(-1)^{q'-q}\right]\Big].\end{aligned} \tag{30}$$

Next I will choose $m = m'$ so that ω_d no longer contributes to any frequency. Then, I examine the four cases when $m = m' = \pm 1$ and $m'' = \pm 1$. These calculations are located in the appendix in B. I

 doi:10.20944/preprints202409.0474.v1

know from the RK4 and diagonalizing the Hamiltonian that for σ_y, the anomalous peaks are for odd q. Choosing odd q, then varying q' (which dictates whether $q'-q$ is even or odd), I have

$$\begin{aligned}
&\sum_{q\geq 0,\,\text{odd}} \frac{1}{2}\left[e^{iq\omega t}+e^{-iq\omega t}\right] iy \\
&\times\Bigg\{\sum_{q'\,\text{odd},q'-q\,\text{even}}\Bigg[\frac{J_{q'}(x)J_{q'-q}(x)+J_{q'}(x)J_{q'-q}(x)}{q'} \\
&\quad+\frac{-J_{q'-q}(x)J_{q'}(x)-J_{q'-q}(x)J_{q'}(x)}{q'-q}\Bigg] \\
&+\sum_{q'\,\text{even},q'-q\,\text{odd}}\Bigg[\frac{-J_{q'}(x)J_{q'-q}(x)-J_{q'}(x)J_{q'-q}(x)}{q'} \\
&\quad+\frac{-J_{q'-q}(x)J_{q'}(x)-J_{q'-q}(x)J_{q'}(x)}{q'-q}\Bigg]\Bigg\} \\
&=iy\sum_{q\geq 0,\,\text{odd}}\cos q\omega t \\
&\times\Bigg\{\sum_{q'\,\text{odd},q'-q\,\text{even}}\Bigg[\frac{J_{q'}(x)J_{q'-q}(x)+J_{q'}(x)J_{q'-q}(x)}{q'} \\
&\quad+\frac{-J_{q'-q}(x)J_{q'}(x)-J_{q'-q}(x)J_{q'}(x)}{q'-q}\Bigg] \\
&+\sum_{q'\,\text{even},q'-q\,\text{odd}}\Bigg[\frac{-J_{q'}(x)J_{q'-q}(x)-J_{q'}(x)J_{q'-q}(x)}{q'} \\
&\quad+\frac{-J_{q'-q}(x)J_{q'}(x)-J_{q'-q}(x)J_{q'}(x)}{q'-q}\Bigg]\Bigg\},
\end{aligned} \tag{31}$$

with $J_{q'}(x)$ and $J_{q'-q}(x)$ commuting. Of the four terms in Equation 31, the first and the fourth will be equal but opposite sign for certain q and q' values. Whereas the second and the third will be equal and same sign. I will show two examples of this when $q=1$ and I choose different values of q' based off the sum rules in Appendix C.

Finally, the expectation value for $m=m'$ and odd q can be written as

$$\begin{aligned}
&<\sigma_y(t)>|_{m=m'} \\
&=-4iy\sum_{q>0,\text{odd}}\sum_{q'\neq 0,\text{even}}\cos q\omega t\frac{J_{q'-q}(x)J_{q'}(x)}{q'}.
\end{aligned} \tag{32}$$

The first few terms are

$$\begin{aligned}
&-4iy\Bigg[\cos\omega t\frac{J_1(x)J_2(x)}{(2)}+\cos\omega t\frac{J_{-3}(x)J_{-2}(x)}{(-2)} \\
&+\cos 3\omega t\frac{J_{-1}(x)J_2(x)}{(2)}+\cos 3\omega t\frac{J_{-5}(x)J_{-2}(x)}{(-2)}+...\Bigg] \\
&=-2iyJ_2(x)\Bigg[\left[J_1(x)+J_3(x)\right]\cos\omega t \\
&\quad+\left[J_5(x)-J_1(x)\right]\cos 3\omega t+...\Bigg].
\end{aligned} \tag{33}$$

For all the other cases ($m\neq m'$ with q odd or even and $m=m'$ with even q) all terms vanish.

Preprints.org (www.preprints.org) | NOT PEER-REVIEWED | Posted: 5 September 2024 doi:10.20944/preprints202409.0474.v1

For σ_z, the matrix elements are

$$\begin{aligned}
&\overline{\langle n', m'|}\sigma_z\overline{|n, m\rangle} = \frac{1}{2}\Big[\big[\langle +|\overline{\langle n'_+|} - im'\langle -|\overline{\langle n'_-|}\big] \\
&+yA'^{*}\big[\langle +|\overline{\langle n''_+|} - im''\langle -|\overline{\langle n''_-|}\big]\Big] \times \big[-i|+\rangle\langle -| + i|-\rangle\langle +|\big] \\
&\times\Big[\big[\overline{|n_+\rangle}|+\rangle + im\overline{|n_-\rangle}|-\rangle\big] + yA\big[\overline{|n''_+\rangle}|+\rangle + im''\overline{|n''_-\rangle}|-\rangle\big]\Big] \\
&= \frac{1}{2}\Big[m\overline{\langle n'_+|n_-\rangle} + m'\overline{\langle n'_-|n_+\rangle} + yA'^{*}\Big[m\overline{\langle n''_+|n_-\rangle} + m''\overline{\langle n''_-|n_+\rangle}\Big] \\
&+yA\Big[m'\overline{\langle n'_-|n''_+\rangle} + m''\overline{\langle n'_+|n''_-\rangle}\Big] + O(y^2)\Big] \\
&= \frac{1}{2}\Big[mJ_q(x)(-1)^q + m'J_q(x) \\
&+yA'^{*}\Big[mJ_{q'}(x)(-1)^{q'} + m''J_{q'}(x)\Big] \\
&+yA\Big[m'J_{q'-q}(x) + m''J_{q'-q}(x)(-1)^{q'-q}\Big] + O(y^2)\Big].
\end{aligned} \tag{34}$$

So that the expectation value up to y is

$$\begin{aligned}
&< \sigma_z(t) >= \sum_{m,m',m''}\sum_{q,q'}\frac{1}{2}a^*_{n'}a_n e^{iq\omega t}e^{i(m-m')\omega_d t/2} \\
&\times\Big[mJ_q(x)(-1)^q + m'J_q(x) + myA'^{*}J_{q'}(x)(-1)^{q'} + m''yA'^{*}J_{q'}(x) \\
&+m'yAJ_{q'-q}(x) + m''yAJ_{q'-q}(x)(-1)^{q'-q}\Big].
\end{aligned} \tag{35}$$

This time, I'll exclude the zeroth order terms. The calculation for the sum over spins for $m = m'$ is similar to the σ_y calculation. Then the linear in y terms are

$$\begin{aligned}
&< \sigma_z(t) > \\
&= \sum_{q,q'}\frac{1}{2}e^{iq\omega t}y\Big[\frac{J_{q'-q}(x)(-1)^{q'-q}J_{q'}(x)(-1)^{q'} + J_{q'-q}(x)J_{q'}(x)}{q'-q} \\
&+\frac{J_{q'}(x)(-1)^{q'}J_{q'-q}(x) + J_{q'}(x)J_{q'-q}(x)(-1)^{q'-q}}{q'}\Big].
\end{aligned} \tag{36}$$

 doi:10.20944/preprints202409.0474.v1

For $\sigma_z(t)$, I saw the anomalies are for even q. Then I have

$$\begin{aligned}
&< \sigma_z(t) >= \sum_{q\geq 0,\text{even}} \frac{1}{2}\left[e^{iq\omega t} + e^{-iq\omega t}\right] y \\
&\times \Bigg\{ \sum_{q' \text{ odd}, q'-q \text{ odd}} \Bigg[\frac{J_{q'-q}(x)J_{q'}(x) + J_{q'-q}(x)J_{q'}(x)}{q'-q} \\
&\quad + \frac{-J_{q'}(x)J_{q'-q}(x) - J_{q'}(x)J_{q'-q}(x)}{q'} \Bigg] \\
&+ \sum_{q' \text{ even}, q'-q \text{ even}} \Bigg[\frac{J_{q'-q}(x)J_{q'}(x) + J_{q'-q}(x)J_{q'}(x)}{q'-q} \\
&\quad + \frac{J_{q'}(x)J_{q'-q}(x) + J_{q'}(x)J_{q'-q}(x)}{q'} \Bigg] \Bigg\} \\
&= 4y \sum_{q'\neq 0,\text{ odd}} \frac{J^2_{q'}(x)}{q'} \\
&+ 4y \sum_{q>0,\text{even}} \sum_{q'\neq 0,\text{odd}} \cos q\omega t \frac{J_{q'-q}(x)J_{q'}(x)}{q'},
\end{aligned} \tag{37}$$

with the first 4 terms being

$$\begin{aligned}
&4y\Bigg[\frac{J_1(x)J_1(x)}{(2)} + \frac{J_{-1}(x)J_{-1}(x)}{(-1)} - \cos 2\omega t \frac{J_1(x)J_1(x)}{(1)} \\
&\quad - \cos 2\omega t \frac{J_3(x)J_1(x)}{(-1)}\Bigg] \\
&= 4y\Bigg[(\text{oscillatory } q = 0 \text{ term}) \\
&- \cos 2\omega t J_1(x)\left[J_1(x) - J_3(x) + ...\right] + ...\Bigg].
\end{aligned} \tag{38}$$

Regarding σ_x, I saw anomalous frequencies at $q\omega$ and $\omega_d \pm 2\omega$. The matrix elements for σ_x are

 doi:10.20944/preprints202409.0474.v1

$$
\begin{aligned}
\overline{\langle n', m'|}\sigma_x\overline{|n, m\rangle} &= \frac{1}{2}\Big[\big[\langle +|\overline{\langle n'_+|} - im'\langle -|\overline{\langle n'_-|}\big] \\
&+ yA'^{*}\big[\langle +|\overline{\langle n''_+|} - im''\langle -|\overline{\langle n''_-|}\big]\Big] \\
&\times\big[|+\rangle\langle +| - |-\rangle\langle -|\big]\Big[\big[\overline{|n_+\rangle}|+\rangle + im\overline{|n_-\rangle}|-\rangle\big] \\
&+ yA\big[\overline{|n''_+\rangle}|+\rangle + im''\overline{|n''_-\rangle}|-\rangle\big]\Big] \\
&= \frac{1}{2}\Big[\big[\langle +|\overline{\langle n'_+|} - im'\langle -|\overline{\langle n'_-|}\big] \\
&+ yA'^{*}\big[{}_x\langle +|\overline{\langle n''_+|} - im''\langle -|\overline{\langle n''_-|}\big]\Big] \\
&\times\Big[\big[\overline{|n_+\rangle}|+\rangle - im\overline{|n_-\rangle}|-\rangle\big] \\
&+ yA\big[\overline{|n''_+\rangle}|+\rangle - im''\overline{|n''_-\rangle}|-\rangle\big]\Big] \\
&= \frac{1}{2}\Big[\overline{\langle n'_+|n_+\rangle} - mm'\overline{\langle n'_-|n_-\rangle} \\
&+ yA'\big[\overline{\langle n''_+|n_+\rangle} - mm''\overline{\langle n''_-|n_-\rangle}\big] \\
&+ yA\big[\overline{\langle n'_+|n''_+\rangle} - m'm''\overline{\langle n'_-|n''_-\rangle}\big] + O(y^2)\Big] \\
&= \frac{1}{2}\Big[(1 - mm')\delta_{n,n'} \\
&+ yA'(1 - mm'')\delta_{n,n''} + yA(1 - m'm'')\delta_{n',n''}\Big],
\end{aligned}
\tag{39}
$$

so that the expectation value is

$$
\begin{aligned}
< \sigma_x(t) > = &\sum_{m,m',m''}\sum_{n,n',n''}\frac{1}{2}a^*_{n'}a_n e^{iq\omega t}e^{i(m-m')\omega_d t/2} \\
&\times\Big[(1 - mm')\delta_{n,n'} \\
&+ yA'(1 - mm'')\delta_{n,n''} + yA(1 - m'm'')\delta_{n',n''}\Big].
\end{aligned}
\tag{40}
$$

For summing over all n's and m's in Equation 40, I have the following cases and their constraints (due to $k \neq n$ in the formulation for first order perturbation theory)

$$
\begin{aligned}
&n = n', \quad n'' \neq n \rightarrow n'' \neq n' \rightarrow \text{no } m \text{ constraints;} \\
&n = n', \quad n'' = n \rightarrow n'' = n' \rightarrow m'' \neq m', \quad m'' \neq m; \\
&n \neq n', \quad n'' \neq n \rightarrow n'' = n' \rightarrow m'' \neq m'; \\
&n \neq n', \quad n'' = n \rightarrow n'' \neq n' \rightarrow m'' \neq m.
\end{aligned}
\tag{41}
$$

 doi:10.20944/preprints202409.0474.v1

Of these four cases, the first leads to the zeroth order $\cos\omega_d t$ term. The second case has $q' = 0$ and $q' - q = 0$ which is not allowed. Cases three and four are the ones I care about. Given I'm in a spin $1/2$ system, a constraint like $m'' \neq m'$ means $m'' = -m$ and so I can simply replace all m'''s by $-m$. Also, the third case has $q' - q = 0$ so that any q' can be replaced by q. And the fourth case has $q' = 0$ but given $n'' \neq n'$, there's no singularity. The calculation for the third case is

$$\begin{aligned}
&\sum_{m,m',m''}\sum_{n,n'}\frac{1}{2}a^*_{n'}a_n e^{iq\omega t}e^{i(m-m')\omega_d t/2}y\\
&\times\frac{mJ_q(x)(-1)^q + m''J_q(x)}{4(q)}[1 - m'm'']\\
&= \sum_q\sum_{m,m'}\frac{1}{2}e^{iq\omega t}e^{i(m-m')\omega_d t/2}y\\
&\times\frac{mJ_q(x)(-1)^q - m'J_q(x)}{4q}[1 + (m')^2]\\
&= y\sum_q e^{iq\omega t}\frac{J_q(x)}{4q}\Big[\Big[(-1)^q - 1\Big] + e^{-i\omega_d t}\Big[-(-1)^q - 1\Big]\\
&\quad + e^{i\omega_d t}\Big[(-1)^q + 1\Big] + \Big[-(-1)^q + 1\Big]\Big]\\
&= y\sum_q e^{iq\omega t}\frac{J_q(x)}{4q}\Big[(-1)^q + 1\Big]\Big[e^{i\omega_d t} - e^{-i\omega_d t}\Big]\\
&= y\sum_{q>0,\text{even}}\Big[e^{iq\omega t} + e^{-iq\omega t}\Big]\frac{J_q(x)}{4q}(2)(2i\sin\omega_d t)\\
&= 2iy\sum_{q>0,\text{even}}\frac{J_q(x)}{q}\cos q\omega t\sin\omega_d t.
\end{aligned} \tag{42}$$

 doi:10.20944/preprints202409.0474.v1

And the fourth case

$$\begin{aligned}
&\sum_{m,m',m''}\sum_{n,n'}\frac{1}{2}a^*_{n'}a_n e^{iq\omega t}e^{i(m-m')\omega_d t/2}y\\
&\times\frac{m'J_{q'-q}(x)(-1)^{q'-q}+m''J_{q'-q}(x)}{4(q'-q)}[1-mm'']\\
&=\sum_q\sum_{m,m'}\frac{1}{2}e^{iq\omega t}e^{i(m-m')\omega_d t/2}y\\
&\times\frac{m'J_{-q}(x)(-1)^{-q}-mJ_{-q}(x)}{4(-q)}[1+m^2]\\
&=-y\sum_q\sum_{m,m'}e^{iq\omega t}e^{i(m-m')\omega_d t/2}\frac{m'J_q(x)-mJ_q(x)(-1)^q}{2q}\\
&=-\frac{1}{2}y\sum_q e^{iq\omega t}\frac{J_q(x)}{2q}\Big[\Big[1-(-1)^q\Big]+e^{-i\omega_d t}\Big[1+(-1)^q\Big]\\
&\quad+e^{i\omega_d t}\Big[-1-(-1)^q\Big]+\Big[-1+(-1)^q\Big]\Big]\\
&=-y\sum_q e^{iq\omega t}\frac{J_q(x)}{4q}\Big[1+(-1)^q\Big]\Big[e^{-i\omega_d t}-e^{i\omega_d t}\Big]\\
&=-y\sum_{q>0,\text{even}}\Big[e^{iq\omega t}+e^{-iq\omega t}\Big]\frac{J_q(x)}{4q}(2)(-2i\sin\omega_d t)\\
&=2iy\sum_{q>0,\text{even}}\frac{J_q(x)}{q}\cos q\omega t\sin\omega_d t.
\end{aligned}\tag{43}$$

Adding together the results from the third and fourth cases gives the full linear in y dependence of σ_x as

$$4iy\sum_{q>0,\text{even}}\frac{J_q(x)}{q}\cos q\omega t\sin\omega_d t.\tag{44}$$

From the results of Equation 44, it can be seen that the σ_x $\omega_d \pm q\omega$ for even q, anomaly has be resolved. Also just as important is that the $q\omega$ anomaly did not show itself since data in the earlier section suggested it would depend on y^2. The y^2 terms from the first order corrections that I ignored plus the y^2 terms that would come about in second order corrections should show the frequencies $q\omega$ for odd q. The plots with the first order corrections added to the theory, analogous to Figures 2 to 4 are shown below in Figures 15 to 17.

 doi:10.20944/preprints202409.0474.v1

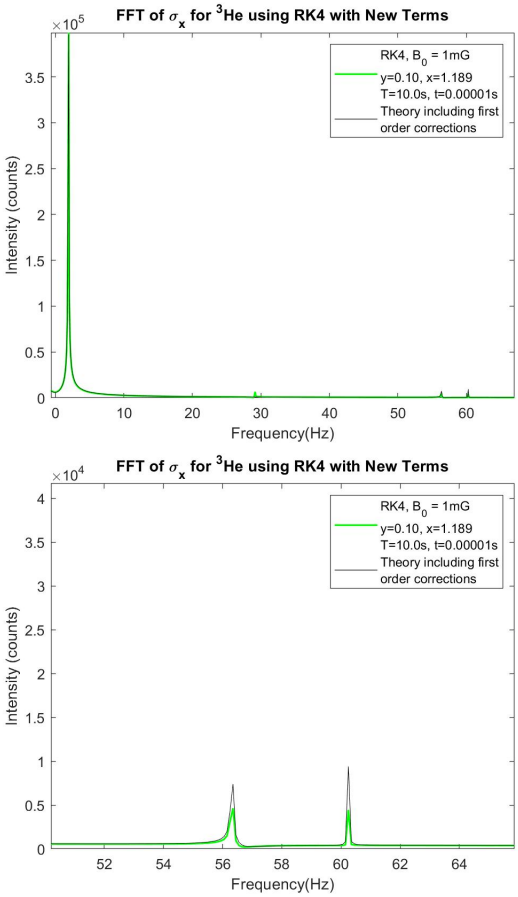

Figure 15. σ_x for $y = 0.10$, frequencies solved for using the RK4 method. The $\omega_d \pm 2\omega$ frequencies are now accounted for with the first order corrections to the eigenstates. The bottom plot shows the anomalies with a zoomed-in view.

 doi:10.20944/preprints202409.0474.v1

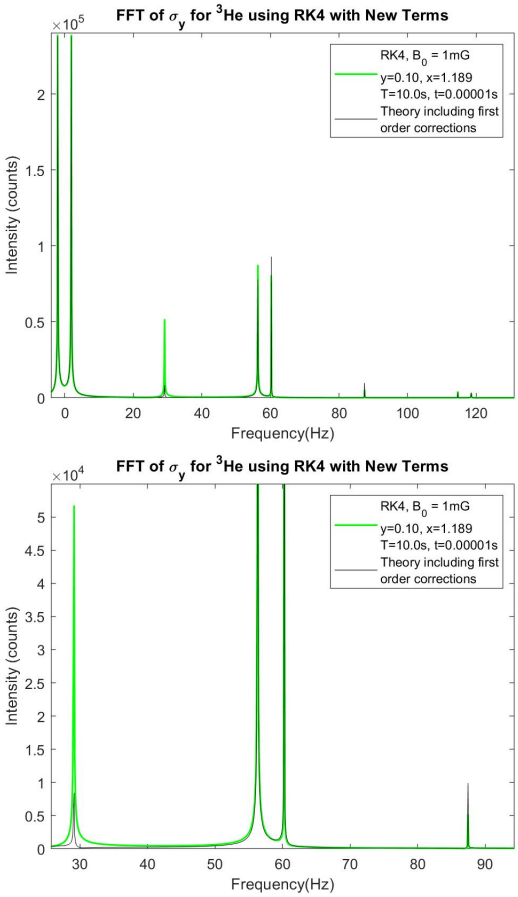

Figure 16. σ_y for $y = 0.10$, frequencies solved for using the RK4 method. The ω and 3ω frequencies are now accounted for with the first order corrections to the eigenstates. The bottom plot shows the anomalies with a zoomed-in view.

 doi:10.20944/preprints202409.0474.v1

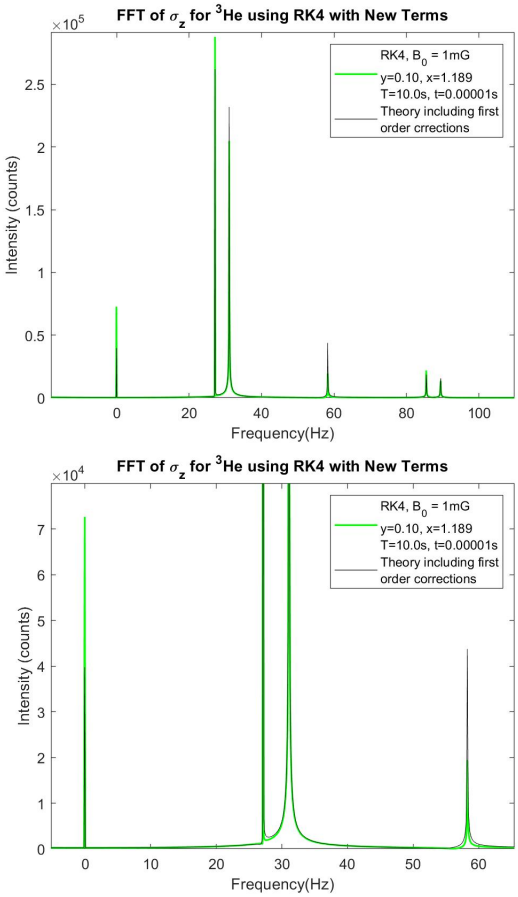

Figure 17. σ_y for $y = 0.10$, frequencies solved for using the RK4 method. The 0ω and 2ω frequencies are now accounted for with the first order corrections to the eigenstates. The bottom plot shows the anomalies with a zoomed-in view.

In Figure 15, the $\omega_d \pm 2\omega$ theoretical heights in black from the first order corrections are too large. In Figure 16, the ω theory peak is too small while the 3ω is too large. Figure 17 has discrepancies between RK4 heights and the new terms added to the theory as well. I also simply used 0.10 as a placeholder for the $q = 0$ oscillatory term. The differences are most likely due to either factors of 2 missing for certain frequency amplitudes, missing Bessel function terms since I stopped the sums after two terms or issues with normalization for Fourier transforms in Matlab.

What has been demonstrated is that the J_0 approximation is not valid for $y = 0.10$ considering the non-negligible intensities in the σ_y and σ_z FFTs. The next section will show that again, when using $y = 0.10$, perturbation theory needs to be extended for the eigenvalues as well.

5. The Critical Dressing Condition

Critical dressing is defined by when the precession rate about the z-axis is matched between the two particle species. In regards of UCN and ^{3}He, this means matching their effective Larmor frequencies. From earlier, the normal Larmor frequencies $\omega_0 = -\gamma B_0$ has been shifted by a factor of $J_0(x)$. Then the critical dressing condition is:

$$-\gamma_n B_0 [J_0(x_c) - \alpha J_0(\alpha x_c)] = 0, \tag{45}$$

where $x_c = \omega_1/\omega$ is the critical dressing parameter and has been chosen to satisfy Equation 45 by adjusting the magnitude of the oscillating field B_1. Thus, the condition is defined using the first order corrections to the eigenvalues. When I mentioned the J_0 approximation last section, this is precisely what the approximation says: the first order corrections to the eigenvalues are sufficient. However, I

 doi:10.20944/preprints202409.0474.v1

found in my simulations that the critical dressing parameter was varying drastically from the solution to Equation 45. Not only that but x_c also had y^2 dependence. Furthermore, the reason I investigated further into the critical dressing condition is because I wanted to perform simulations where a ^{3}He pseudomagnetic field would be modulated via the dressing field and its affect nullified. If the critical dressing parameter changes, the point where the modulation centers on changes. A plot of $J_0(x)$ is shown in Figure 18 and the absolute value of the critical dressing condition is shown in Figure 19.

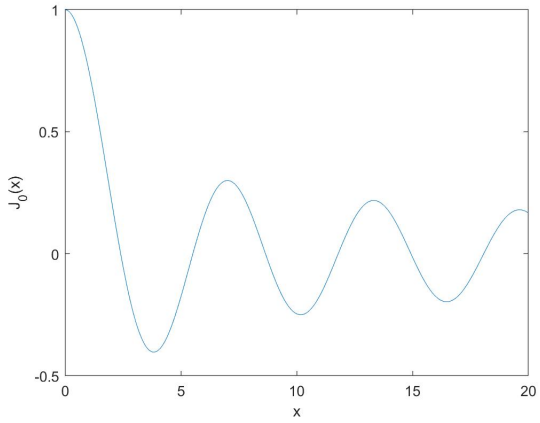

Figure 18. The zeroth order Bessel function of the first kind.

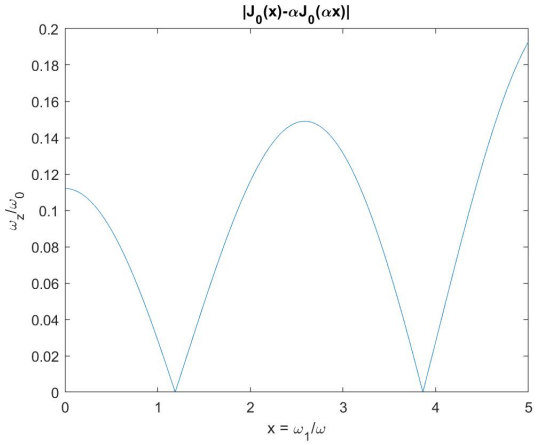

Figure 19. The absolute value of the critical dressing condition where the y-axis is the relative frequency between UCN and ^{3}He, ω_z, divided by ω_0.

The first zero is at the critical dressing point the experiment will use because the nEDM term gets diluted by the Bessel function correction so the largest value of $J_0(x)$ should be used. This solution in the J_0 approximation is $x_c = 1.189018$. When I performed simulations where I solved for x_c using the same field parameters as the experiment ($B_0 = 30$ mG, $y = 0.10$), critical dressing was at $x_c = 1.18246$.... This 0.55% difference between my simulation value and the analytical J_0 approximation value was the first indication that something was missing. The second indication was when I tried modulating the dressing field. When the dressing field is set for critical dressing, the neutrons and Helium precess about the z-axis at the same rate. Since dressing is controlling the relative rate, a change in x has the

 doi:10.20944/preprints202409.0474.v1

effect, when averaged over, of producing a $\delta\omega$ about the z-axis between the UCN and ^{3}He. The Bessel function is asymmetric about critical dressing so I will label the $\delta\omega$'s as ω_{z1} and ω_{z2}

$$\begin{aligned} B_{rf1} &= (x_c + x_m)\omega/\gamma_n \\ B_{rf2} &= (x_c - x_m)\omega/\gamma_n \\ \omega_{z1} &= -\gamma B_0[J_0(x_c + x_m) - \alpha J_0(\alpha(x_c + x_m))] \\ \omega_{z2} &= -\gamma B_0[J_0(x_c - x_m) - \alpha J_0(\alpha(x_c - x_m))] \end{aligned} \tag{46}$$

where I will write B_1 as B_{rf} going forward since there will be two different magnitudes of the dressing field. Intuitively, ω_{z1} being near the magnitude of ω_{z2} should give symmetry about critical dressing. This would make sense since the UCN and ^{3}He need to alternate relative phase shifts in a symmetric manner while J_0 itself is asymmetric as mentioned. The data I looked at for symmetry was the scintillation signal which the experiment relies on. This signal is maximum when there's a maximum component of anti-parallel spins between the two species (Appendix D talks about the spin dependent scattering length of of neutron-^{3}He capture which leads to a periodic scintillation rate and a pseudomagnetic field). Therefore, observing the behavior of $\vec{\sigma}_3 \cdot \vec{\sigma}_n$ with modulation gives evidence as to whether the modulation is doing a good enough job to offset the pseudomagnetic field. But what I first saw was that $\omega_{z1} \approx |\omega_{z2}|$ was leading to large asymmetries in $\vec{\sigma}_3 \cdot \vec{\sigma}_n$ as shown in Figure 20.

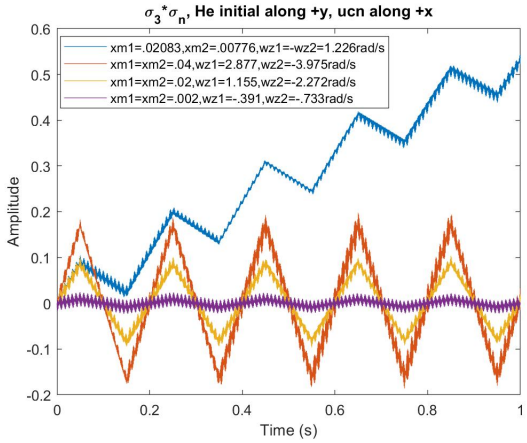

Figure 20. $\vec{\sigma}_3 \cdot \vec{\sigma}_n$ vs time with $\omega_{z1} = -\omega_{z2}$ in blue and $x_{m1} = x_{m2}$ in orange, yellow and purple. The two cases are mutually exclusive.

Note, in most of my simulations, the initial conditions have the spin parallel to each other. However Figure 20 has the spins initially perpendicular so that the symmetry or asymmetry about 0 can be seen easier. As can be seen, the blue curve which had $\omega_{z1} = -\omega_{z2}$, was asymmetric about 0 and therefore continuously had phase shifts building. Whereas the three other curves for $x_{m1} = x_{m2}$ are mostly symmetric about 0. What this points to given the definition of ω_z is that the expressions for $\omega_{z1,2}$ are wrong. This can be conceptualized by thinking about why symmetric x_m is leading to $\vec{\sigma}_3 \cdot \vec{\sigma}_n$ symmetry. Looking at Figure 19, symmetric x_m ($x_{m1} \approx x_{m2}$) for x_m small should lead to $\omega_{z1} \approx |\omega_{z2}|$. But as can be seen in the legend of Figure 20, ω_1 and ω_2 have large percentage differences. This led me to think back to whether the J_0 approximation is valid for $y = 0.10$ and the idea of extending the eigenvalues to higher orders.

 doi:10.20944/preprints202409.0474.v1

6. Corrections to the Eigenvalues

The general expression for the second order correction to the eigenvalues is

$$E^{(2)} = \lambda^2 \sum_{k \neq n} \frac{|\left\langle k^{(0)} \right| V \left| n^{(0)} \right\rangle|^2}{E_n^{(0)} - E_k^{(0)}}, \tag{47}$$

and using the bar eigenstates of m_z where $m_z = \pm\frac{1}{2} = \pm\frac{m}{2}$

$$\begin{aligned} E^{(2)} &= \frac{\omega_0^2}{4} \sum_{n'm'} \frac{|\overline{\langle n', m'|} \sigma_z \overline{|n, m\rangle}|^2}{(n - n')\omega} \\ &= \frac{y\omega_0}{16} \sum_{m', q \neq 0} \frac{\left[m J_q(x)(-1)^q + m' J_q(x) \right]^2}{q} = 0. \end{aligned} \tag{48}$$

Next are the third order corrections to the eigenvalues which I suspected to be the source. The third order corrections to the eigenvalues have two summation terms and one is easier to calculate than the other. The general expression is

$$\begin{aligned} E_n^{(3)} = \sum_{k \neq n} \sum_{m \neq n} \frac{\left\langle n^{(0)} \right| V \left| m^{(0)} \right\rangle \left\langle m^{(0)} \right| V \left| k^{(0)} \right\rangle \left\langle k^{(0)} \right| V \left| n^{(0)} \right\rangle}{(E_n^{(0)} - E_m^{(0)})(E_n^{(0)} - E_k^{(0)})} \\ - \left\langle n^{(0)} \right| V \left| n^{(0)} \right\rangle \sum_{m \neq n} \frac{|\left\langle n^{(0)} \right| V \left| m^{(0)} \right\rangle|^2}{(E_n^{(0)} - E_m^{(0)})^2}. \end{aligned} \tag{49}$$

Defining $V_{nm,n'm'} = \overline{\langle n', m'|} \frac{1}{2} \omega_0 \sigma_z \overline{|n, m\rangle}$, the third order correction in this context is

$$\begin{aligned} E_n^{(3)} = \sum_{n', m' \neq n, m} \sum_{n'', m'' \neq n, m} \frac{V_{n''m'', nm} V_{n'm', n''m''} V_{nm, n'm'}}{(n\omega - n''\omega)(n\omega - n'\omega)} \\ - V_{nm,nm} \sum_{n', m' \neq n, m} \frac{|V_{nm,n'm'}|^2}{(n\omega - n'\omega)^2}. \end{aligned} \tag{50}$$

The Physics Reports [1] made the approximation that the first term, which is more complicated than the second, is equal in magnitude as the second term and therefore did not calculate it. What I found is that the first term is actually larger than the second term and when included in the critical dressing condition, produces much better convergence with simulation values. The calculation for the second term in Equation 50 is

$$\begin{aligned} & - \overline{\langle n, m|} \frac{1}{2} \omega_0 \sigma_z \overline{|n, m\rangle} \sum_{n', m' \neq n, m} \frac{|\overline{\langle n', m'|} \frac{1}{2} \omega_0 \sigma_z \overline{|n, m\rangle}|^2}{(n\omega - n'\omega)^2} \\ &= - \frac{\omega_0}{4} [m J_0(x) + m J_0(x)] \sum_{q, m'} \frac{|\frac{\omega_0}{4} [m J_q(x)(-1)^q + m' J_q(x)]|^2}{(q\omega)^2} \\ &= - \frac{1}{32} m \omega_0 J_0(x) y^2 \sum_{q, m'} \frac{[m J_q(x)(-1)^q + m' J_q(x)]^2}{q^2}, \end{aligned} \tag{51}$$

 doi:10.20944/preprints202409.0474.v1

such that for different q's, $m' = m$ or $m' \neq m$. The terms up to $J_3(x)$ are

$$\sum_{m'=\pm m}\Bigg[\frac{[-mJ_1(x)+m'J_1(x)]^2}{(1)^2}+\frac{[mJ_1(x)-m'J_1(x)]^2}{(-1)^2} +\frac{[mJ_2(x)+m'J_2(x)]^2}{(2)^2}+\frac{[mJ_2(x)+m'J_2(x)]^2}{(-2)^2} +\frac{[-mJ_3(x)+m'J_3(x)]^2}{(3)^2}+\frac{[mJ_3(x)-m'J_3(x)]^2}{(-3)^2}+...\Bigg], \tag{52}$$

so that the result is

$$\begin{aligned}&=-\frac{1}{4}m\omega_0 J_0(x)y^2\left[J_1^2(x)+\frac{J_2^2(x)}{4}+\frac{J_3^2(x)}{9}+...\right]\\&=-\frac{1}{2}m_z\omega_0 J_0(x)y^2\left[J_1^2(x)+\frac{J_2^2(x)}{4}+\frac{J_3^2(x)}{9}+...\right].\end{aligned} \tag{53}$$

For the calculation of the first term in Equation 50, first I would like to consider the terms that contain $J_0(x)$ since they will be similar in magnitude to the result in Equation 53. The only way to get a $J_0(x)$ in the first term is for $m = k$ which means $n' = n''$ (but with $m' = \pm m''$) giving

$$\begin{aligned}&\sum_{n',m'\neq n,m}\sum_{n'',m''\neq n,m}\frac{V_{n''m'',nm}V_{n'm',n''m''}V_{nm,n'm'}}{(n\omega-n''\omega)(n\omega-n'\omega)}\\&=\sum_{n',m'\neq n,m}\sum_{m''}\frac{\overline{\langle n,m|}\frac{1}{2}\omega_0\sigma_z\overline{|n',m''\rangle\langle n',m''|}\frac{1}{2}\omega_0\sigma_z\overline{|n',m'\rangle\langle n',m'|}\frac{1}{2}\omega_0\sigma_z\overline{|n,m\rangle}}{(n\omega-n'\omega)(n\omega-n'\omega)}\\&=\frac{1}{64}\omega_0 y^2\sum_{n',m'\neq n,m}\sum_{m''}\\&\frac{[mJ_{-q}(x)+m''J_{-q}(x)(-1)^{-q}](2)[m'J_0(x)+m''J_0(x)][mJ_q(x)(-1)^q+m'J_q(x)]}{q^2}\\&=\frac{1}{32}\omega_0 J_0(x)y^2\sum_{m',q\neq 0}\sum_{m''}\\&\frac{[mJ_{-q}(x)+m''J_{-q}(x)(-1)^{-q}][m'+m''][mJ_q(x)(-1)^q+m'J_q(x)]}{q^2}\\&=\frac{1}{16}\omega_0 J_0(x)y^2\sum_{m',q\neq 0}\frac{m'[mJ_q(x)(-1)^q+m'J_q(x)]^2}{q^2},\end{aligned} \tag{54}$$

where the sum over m'' made $m'' = m'$ or else the whole term vanishes. Continuing the calculation of just the sum

$$\begin{aligned}&\sum_{m',q\neq 0}\frac{m'[mJ_q(x)(-1)^q+m'J_q(x)]^2}{q^2}\\&=\sum_{m'}\Bigg[\frac{m'[-mJ_1(x)+m'J_1(x)]^2}{1^2}+\frac{m'[mJ_1(x)-m'J_1(x)]^2}{(-1)^2} +\frac{m'[mJ_2(x)+m'J_2(x)]^2}{2^2}+\frac{m'[mJ_2(x)+m'J_2(x)]^2}{(-2)^2} +\frac{m'[-mJ_3(x)+m'J_3(x)]^2}{3^2}+\frac{m'[mJ_3(x)-m'J_3(x)]^2}{(-3)^2}+...\Bigg]\\&=\left[\frac{-16m^3J_1^2(x)}{1}+\frac{16m^3J_2^2(x)}{4}+\frac{-16m^3J_3^2(x)}{9}+...\right].\end{aligned} \tag{55}$$

The summation over m' is simply a summation of $m' = m$ and $m' = -m$. Then substituting $m = 2m_z$ as before, the final result for the first term in Equation 50 is

$$\begin{aligned}&\frac{1}{32}\omega_0 J_0(x)y^2\sum_{m',m'',q\neq 0}\frac{[mJ_q(x)(-1)^q+m'J_q(x)]^2[m'+m'']}{q^2}\\&=m_z\omega_0 J_0(x)y^2\left[-J_1^2(x)+\frac{J_2^2(x)}{4}-\frac{J_3^2(x)}{9}+...\right].\end{aligned} \tag{56}$$

Preprints.org (www.preprints.org) | NOT PEER-REVIEWED | Posted: 5 September 2024 doi:10.20944/preprints202409.0474.v1

The new critical dressing condition is

$$
\begin{aligned}
(\omega_n - \omega_3) = 0 = (-\gamma B_0)\Big[& J_0(x_c) - \alpha J_0(\alpha x_c) \\
& - J_0(x_c)\frac{y^2}{2}\big[J_1^2(x_c) + \frac{J_2^2(x_c)}{4} + \frac{J_3^2(x_c)}{9} + ...\big] \\
& + \alpha^3 J_0(\alpha x_c)\frac{y^2}{2}\big[J_1^2(\alpha x_c) + \frac{J_2^2(\alpha x_c)}{4} + \frac{J_3^2(\alpha x_c)}{9} + ...\big] \\
& + J_0(x) y^2\big[- J_1^2(x_c) + \frac{J_2^2(x_c)}{4} - \frac{J_3^2(x_c)}{9} ...\big] \\
& - \alpha^3 J_0(x_c) y^2\big[- J_1^2(\alpha x_c) + \frac{J_2^2(\alpha x_c)}{4} - \frac{J_3^2(\alpha x_c)}{9} + ...\big]\Big] \\
= (-\gamma B_0)\Big[& J_0(x_c) - \alpha J_0(\alpha x_c) \\
& - J_0(x_c)\frac{y^2}{2}\big[3J_1^2(x_c) - \frac{J_2^2(x_c)}{4} + \frac{3J_3^2(x_c)}{9} + ...\big] \\
& + \alpha^3 J_0(\alpha x_c)\frac{y^2}{2}\big[3J_1^2(\alpha x_c) - \frac{J_2^2(\alpha x_c)}{4} + \frac{3J_3^2(\alpha x_c)}{9} + ...\big]\Big].
\end{aligned}
\tag{57}
$$

Now, going back to the other terms that do not include $J_0(x)$, they will either vanish when summed over or be quite small. An example is shown in Appendix E.
Figure 21 shows the zoomed-in view of the new critical dressing condition and how x_c varies for different values of y. This demonstrates how the nEDM experiments needs to account for this shift in x_c not only for the sake of critical dressing and modulating the dressing field but for an accurate expression for the scintillation rate. This third order correction also dilutes the nEDM signal.

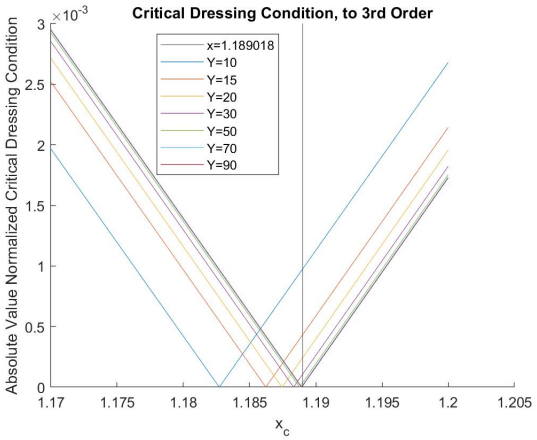

Figure 21. Solutions for critical dressing parameters for different $Y = 1/y$ with the third order corrections as part of the condition. The first line in the legend is just a vertical line for $x = 1.189018$, the solution for critical dressing in the J_0 approximation.

Preprints.org (www.preprints.org) | NOT PEER-REVIEWED | Posted: 5 September 2024 doi:10.20944/preprints202409.0474.v1

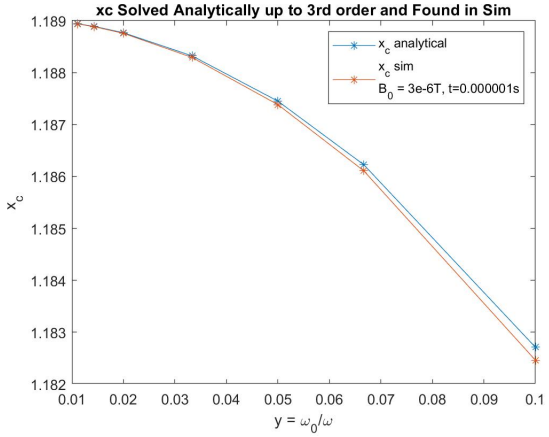

Figure 22. Comparing the analytical critical dressing parameters from Figure 5.12 to those found using the RK4 simulations.

What I now see from my simulations is much better agreement between my simulation x_c and the analytical expression for x_c that includes the third order corrections. Figure 22 shows the analytical and simulation critical dressing parameters for different values of y. And Figure 23 shows the percentage difference of these values at each given value of y. There is still a y^2 dependence in Figure 23 because the third order correction terms I've ignored are of course still proportional to y^2. Given I now have an accurate expression for the critical dressing condition, I can more accurately modulate around it.

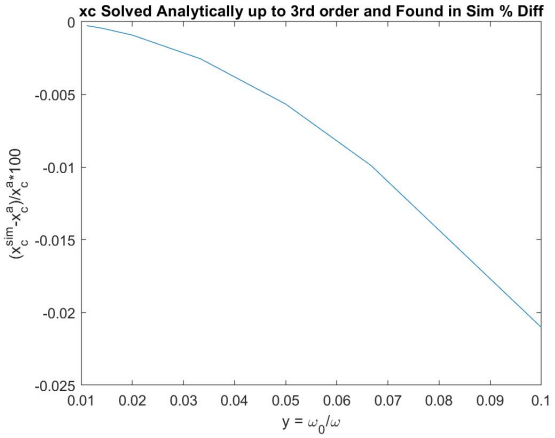

Figure 23. The percentage difference between points in Figure 5.13 for a given Y.

7. Modulation and the Pseudomagnetic Field

With the third order corrections from the last section, I will briefly show what modulation looks like with a pseudomagnetic field on and off. Figure 24 shows a near symmetric scintillation signals with modulation on and an applied pseudomagnetic field off.

 doi:10.20944/preprints202409.0474.v1

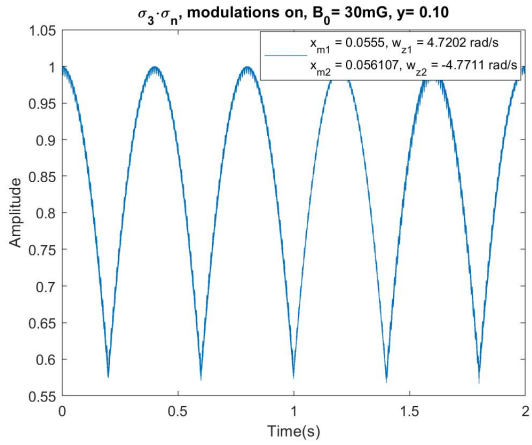

Figure 24. $\vec{\sigma_3} \cdot \vec{\sigma_n}$ vs time for modulation parameters $x_{m1} = 0.0555$ and $x_{m2} = 0.056107$. The scintillation signals are more symmetric than any other modulated $\vec{\sigma_3} \cdot \vec{\sigma_n}$ plot I have shown.

As seen in the legend, the corrected $\omega_{z1,2}$ do have magnitudes much closer to each other than before.

For the magnitude of $\vec{P}$, I wanted to use the value from the paper by Leung et al.[3] where for $x_3 = 10^{-10}$ and $P_3 = 1$ such that $|\vec{P}| \approx 0.10\mu$G. However, this magnitude is very small compared to the fields already present and the sensitivity of the simulation so instead I looked at $|\vec{P}| \approx 10\mu G$. The relevant plots are shown in Figures 25 to 27. For a benchmark, I first show the difference in $\vec{\sigma_3} \cdot \vec{\sigma_n}$ for the pseudomagnetic field off and on without modulation. Followed by plots where modulation will cancel out the effects from $\vec{P}$. Note that in Figure 25, I chose to use the color blue for the pseudomagnetic field on and orange for it off which differs from other plots. This was solely to give a better contrast to the naked eye.

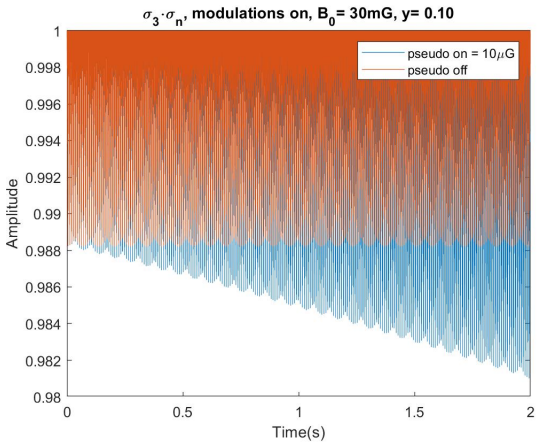

Figure 25. $\vec{\sigma_3} \cdot \vec{\sigma_n}$ vs time for no modulation and the pseudomagnetic field off (orange) and on (blue). The magnitude of $\vec{P}$ is about 100 times larger than in the experiment.

Preprints.org (www.preprints.org) | NOT PEER-REVIEWED | Posted: 5 September 2024 doi:10.20944/preprints202409.0474.v1

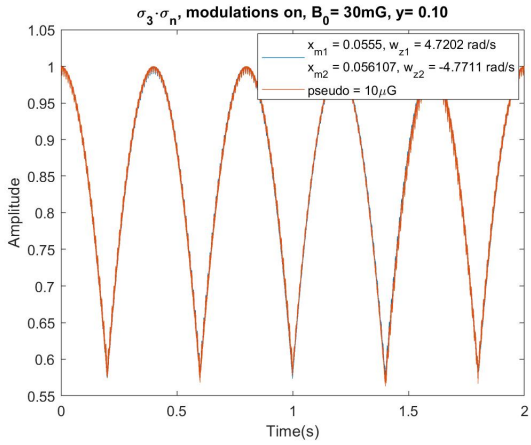

Figure 26. $\vec{\sigma_3} \cdot \vec{\sigma_n}$ vs time with modulation and the pseudomagnetic field off (blue) and on (orange). The magnitude of $\vec{P}$ is about 100 times larger than in the experiment.

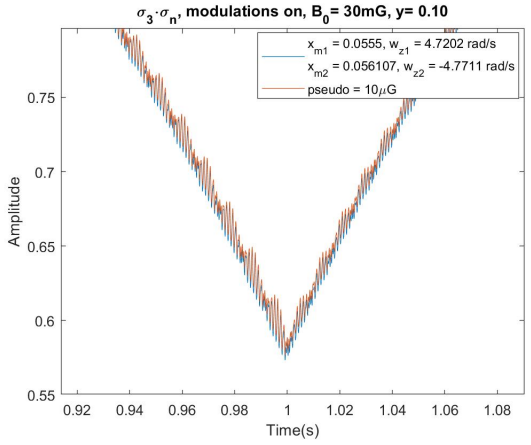

Figure 27. A zoomed-in view of Figure 26 near 1.0 s.

Figure 25 showed that $\vec{P}$ was inducing a non-negligible phase shift between the ^{3}He and UCN that grows linear in time (with no modulation). Then Figures 26 and 27 show the modulation doing a good job at canceling the phase difference that was built in the plots without modulation.

Finally, one way which Robert Golub proposed to quantitatively check how the modulations were performing was to check the relationship between the first and second harmonic signals in Fourier space. The idea is that the first harmonic at 1.25 Hz should be near zero if the modulations are symmetric about x_c. Whereas the second harmonic will have a much larger height and increase in height as the first harmonic signal decreases. So checking the ratio of the second to the first harmonic with modulation on pseudomagnetic field off and modulation on pseudomagnetic field on, will be a better test of whether the modulations are doing their job. I optimized symmetry by looping through x_{m1} values that produced the lowest first harmonic signal. The results were $x_{m1} = 0.05546$ and $x_{m2} = 0.056107$, close to the values I've been using and I used a simulation time of 8 seconds. Figure 28 shows the FFT of $\vec{\sigma_3} \cdot \vec{\sigma_n}$ with modulations, no pseudomagnetic field and zoomed on the modulation harmonics.

Preprints.org (www.preprints.org) | NOT PEER-REVIEWED | Posted: 5 September 2024 doi:10.20944/preprints202409.0474.v1

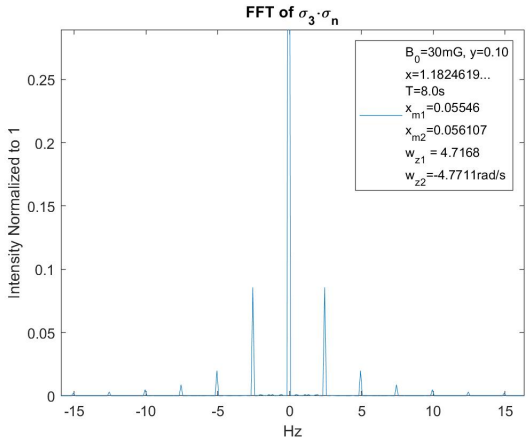

Figure 28. The FFT of $\vec{\sigma_3} \cdot \vec{\sigma_n}$ with modulation, zoomed-in on the harmonics.

The FFTs are shows in Figure 29 where I zoomed-in on the harmonics but further zoomed-in on the first (1.25 Hz) and second (2.5 Hz) harmonics. The colors have been changed to better see where the curves differ and overlap.

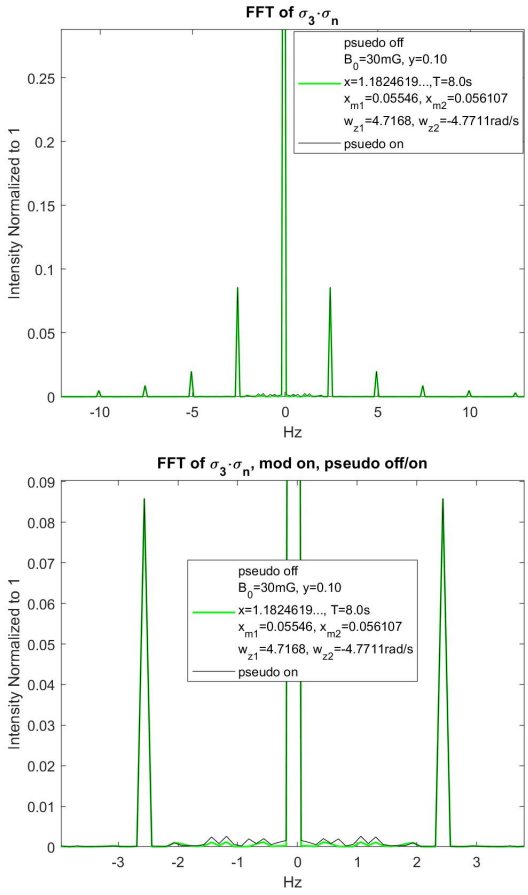

Figure 29. The first and second harmonics. Their ratios are an indicator of how well modulation is working.

The black curve for when the pseudomagnetic field is on has a larger value at the first harmonic which is expected. Due to the binning of the frequency axis which comes from the time steps and length of the simulation, there was no value exactly on 1.25 Hz or 2.5 Hz. For the 1.25 Hz, I took the average of the values at 1.1875 Hz and 1.3125 Hz. For the 2.5 Hz, I used the value at 2.4375 Hz. The results were

 doi:10.20944/preprints202409.0474.v1

that the ratio of the second harmonic signal to the first with the pseudomagnetic field off was 30.055. The ratio with the pseudomagnetic field on was 13.346. Thus, the pseudomagnetic field being flipped to on changed the relative ratios by about a factor of 2.25. This change is a good benchmark as to how well the modulations are doing going forward and with a field that is not 100x the experiment's strength.

Acknowledgments: Thank you to my advisor Robert Golub for his expertise in this field and his direction in where to take my thesis work.

Appendix A. Lifting the Degeneracy

The inner product of two bar states, $\overline{\langle (n-q)_{1/2}||n_{-1/2}\rangle}$, originally done in [2] can be expressed as

$$\begin{aligned}\overline{\langle (n-q)_{1/2}||n_{-1/2}\rangle} &= \langle n-q|e^{\lambda/\omega(a^*-a)}|n\rangle \\ e^{\lambda/\omega(a^*-a)} &= e^{\lambda/\omega a^*}e^{-\lambda/\omega a}e^{-\lambda^2/2\omega^2} \approx e^{\lambda/\omega a^*}e^{-\lambda/\omega a} \\ &\rightarrow \langle n-q|\Big(\sum_m \Big(\frac{\lambda a^*}{\omega}\Big)^m \frac{1}{m!}\Big)\Big(\sum_s \Big(\frac{-\lambda a}{\omega}\Big)^s \frac{1}{s!}\Big)|n\rangle,\end{aligned} \tag{A1}$$

where $\lambda/\omega << 1$. From applying the creation and annihilation operators, you can see the only non-zero result is when $n-q-m = n-s$ so that $m = s-q$. Assume $n >> q,s$ and $q,s >> \omega_1/\omega$, then

$$\begin{aligned}&\sum_s \langle n-q|(-1)^s\Big(\frac{\lambda}{\omega}\Big)^{2s-q}\frac{(a^*)^{s-q}a^s}{(s-q)!s!}|n\rangle \\ &= \sum_s (-1)^s\Big(\frac{\lambda}{\omega}\Big)^{2s-q}\frac{1}{(s-q)!s!} \\ &\times\sqrt{(n-q)(n-q-1)...(n-q-(s-q))}\sqrt{n(n-1)...(n-s)} \\ &\approx \sum_s (-1)^s\Big(\frac{\lambda}{\omega}\Big)^{2s-q}\frac{\sqrt{n}^{2s-q}}{(s-q)!s!} \\ &= \sum_s (-1)^s\Big(\frac{\lambda\sqrt{n}}{\omega}\Big)^{2s-q}\frac{1}{(s-q)!s!} \\ &= J_{-q}\Big(\frac{2\lambda\sqrt{n}}{\omega}\Big) = J_{-q}(\omega_1/\omega)\end{aligned} \tag{A2}$$

where $q = n-n'$, $J_q(x)$ is the Bessel function of the first kind of order q. I substituted $\lambda = \omega_1/2\sqrt{n}$ and a similar calculation for $\overline{\langle n_{1/2}||(n-q)_{-1/2}\rangle}$ has a result of $J_q(\omega_1/\omega)$. Changing the positions of +1/2 or -1/2 changes the sign of the argument.

For a fixed n, the unperturbed states are degenerate in m_x so I want to calculate the matrix elements from the perturbation $\omega_0 s_z$ to lift the degeneracy. I diagonalize this matrix in the x basis to find the eigenvalues and eigenvectors. The sub-matrix elements for a constant n $(q=0)$ are

$$\begin{aligned}\overline{\langle m'_x,n|}\omega_0 s_z\overline{|n,m_x\rangle} &= \langle m'_x|s_z|m_x\rangle\overline{\Big\langle n_{m'_x}\Big|n_{m_x}\Big\rangle}\omega_0 \\ &= \langle m'_x|s_z|m_x\rangle\langle n|e^{(m'_x-m_x)(\lambda/\omega)(a^*-a)}|n\rangle\omega_0 \\ &= \langle m'_x|s_z|m_x\rangle J_0((m'_x-m_x)\omega_1/\omega)\omega_0.\end{aligned} \tag{A3}$$

 doi:10.20944/preprints202409.0474.v1

Given $s_z = m_z\sigma_z$, I want to solve $\langle m'_x|\sigma_z|m_x\rangle$ for all combinations of $m_x = \pm 1$ and $m'_x = \pm 1$. Writing $\sigma_z = -i|+\rangle_{xx}\langle -| + i|-\rangle_{xx}\langle +|$, gives

$$
\begin{aligned}
&{}_{\pm}\langle \pm|\sigma_z|\pm\rangle_x = 0 \\
&{}_x\langle +|\sigma_z|-\rangle_x \\
&=_x \langle +|\left[-i|+\rangle_{xx}\langle -| + i|-\rangle_{xx}\langle +|\right]|-\rangle_x = -i \\
&{}_x\langle -|\sigma_z|+\rangle_x \\
&=_x \langle -|\left[-i|+\rangle_{xx}\langle -| + i|-\rangle_{xx}\langle +|\right]|+\rangle_x = i
\end{aligned}
\tag{A4}
$$

so that the matrix I must diagonalize is

$$
\frac{1}{2}\omega_0\begin{pmatrix} 0 & -iJ_0(\omega_1/\omega) \\ iJ_0(-\omega_1/\omega) & 0 \end{pmatrix} = \frac{1}{2}\omega_0 J_0(\omega_1/\omega)\sigma_z \tag{A5}
$$

The eigenvalues come from the determinant after inserting $-\eta$'s such that the eigenvalue equation and its solution is

$$
\begin{aligned}
\eta^2 - J_0(\omega_1/\omega)J_0(-\omega_1/\omega)\frac{1}{4}\omega_0^2 &= 0 \\
\eta = \pm\frac{1}{2}J_0(\omega_1/\omega)\omega_0 &\equiv m_z\omega_d.
\end{aligned}
\tag{A6}
$$

Equation A6 shows by how much the energy levels are shifted. Solving for the eigenvectors $\vec{k}_1$ and $\vec{k}_2$

$$
\begin{aligned}
\frac{\omega_0}{2}\begin{pmatrix} -J_0(\omega_1/\omega) & -iJ_0(\omega_1/\omega) \\ iJ_0(\omega_1/\omega) & -J_0(\omega_1/\omega) \end{pmatrix} * \vec{k}_1 &= 0 \\
\vec{k}_1 = \frac{1}{\sqrt{2}}\begin{pmatrix} 1 \\ i \end{pmatrix} & \\
\frac{\omega_0}{2}\begin{pmatrix} J_0(\omega_1/\omega) & -iJ_0(\omega_1/\omega) \\ iJ_0(\omega_1/\omega) & J_0(\omega_1/\omega) \end{pmatrix} * \vec{k}_2 &= 0 \\
\vec{k}_2 = \frac{1}{\sqrt{2}}\begin{pmatrix} 1 \\ -i \end{pmatrix} &
\end{aligned}
\tag{A7}
$$

so that both eigenvectors in the bar basis are

$$
\begin{aligned}
\vec{k}_1 &= \frac{1}{\sqrt{2}}(\overline{|n,+\rangle}_x + i\overline{|n,-\rangle}_x) \\
\vec{k}_2 &= \frac{1}{\sqrt{2}}(\overline{|n,+\rangle}_x - i\overline{|n,-\rangle}_x).
\end{aligned}
\tag{A8}
$$

 doi:10.20944/preprints202409.0474.v1

Appendix B. σ_y Expectation Value Selection Rules

The expectation value of σ_y with first order corrections to the eigenstates for $m = m'$ gives the following terms for the expressions in the large bracket of Equation 38

$$
\begin{aligned}
& m = m' = 1, m'' = \pm 1 \\
& e^{iq\omega t}\Big[iJ_q(x)(-1)^q - iJ_q(x) \\
& + iy\frac{[J_{q'-q}(x)(-1)^{q'-q} + m''J_{q'-q}(x)]}{4(q'-q)}[J_{q'}(x)(-1)^{q'} - m''J_{q'}(x)] \\
& + iy\frac{[J_{q'}(x)(-1)^{q'} + m''J_{q'}(x)]}{4q'}[-J_{q'-q}(x) + m''J_{q'-q}(x)(-1)^{q'-q}]\Big] \\
& = e^{iq\omega t}\Big[iJ_q(x)(-1)^q - iJ_q(x) \\
& + iy\frac{[J_{q'-q}(x)(-1)^{q'-q} + J_{q'-q}(x)]}{4(q'-q)}[J_{q'}(x)(-1)^{q'} - J_{q'}(x)] \\
& + iy\frac{[J_{q'}(x)(-1)^{q'} + J_{q'}(x)]}{4q'}[-J_{q'-q}(x) + J_{q'-q}(x)(-1)^{q'-q}]\Big] \\
& + e^{iq\omega t}\Big[iJ_q(x)(-1)^q - iJ_q(x) \\
& + iy\frac{[J_{q'-q}(x)(-1)^{q'-q} - J_{q'-q}(x)]}{4(q'-q)}[J_{q'}(x)(-1)^{q'} + J_{q'}(x)] \\
& + iy\frac{[J_{q'}(x)(-1)^{q'} - J_{q'}(x)]}{4q'}[-J_{q'-q}(x) - J_{q'-q}(x)(-1)^{q'-q}]\Big] \\
& = e^{iq\omega t}\Big[2iJ_q(x)(-1)^q - 2iJ_q(x) \\
& + 2iy\frac{J_{q'-q}(x)(-1)^{q'-q}J_{q'}(x)(-1)^{q'} - J_{q'-q}(x)J_{q'}(x)}{4(q'-q)} \\
& + 2iy\frac{-J_{q'}(x)(-1)^{q'}J_{q'-q}(x) + J_{q'}(x)J_{q'-q}(x)(-1)^{q'-q}}{4q'}\Big]
\end{aligned}
\tag{A9}
$$

$$
\begin{aligned}
& m = m' = -1, m'' = \pm 1 \\
& e^{iq\omega t}\Big[-iJ_q(x)(-1)^q + iJ_q(x) \\
& + iy\frac{[-J_{q'-q}(x)(-1)^{q'-q} + m''J_{q'-q}(x)]}{4(q'-q)}[-J_{q'}(x)(-1)^{q'} - m''J_{q'}(x)] \\
& + iy\frac{[-J_{q'}(x)(-1)^{q'} + m''J_{q'}(x)]}{4q'}[J_{q'-q}(x) + m''J_{q'-q}(x)(-1)^{q'-q}]\Big] \\
& = e^{iq\omega t}\Big[-2iJ_q(x)(-1)^q + 2iJ_q(x) \\
& + 2iy\frac{J_{q'-q}(x)(-1)^{q'-q}J_{q'}(x)(-1)^{q'} - J_{q'-q}(x)J_{q'}(x)}{4(q'-q)} \\
& + 2iy\frac{-J_{q'}(x)(-1)^{q'}J_{q'-q}(x) + J_{q'}(x)J_{q'-q}(x)(-1)^{q'-q}}{4q'}\Big]
\end{aligned}
$$

Adding the terms together between the choices for all m's we have:

$$
\begin{aligned}
& e^{iq\omega t}iy\Big[\frac{-J_{q'}(x)(-1)^{q'}J_{q'-q}(x) + J_{q'}(x)J_{q'-q}(x)(-1)^{q'-q}}{q'} \\
& + \frac{J_{q'-q}(x)(-1)^{q'-q}J_{q'}(x)(-1)^{q'} - J_{q'-q}(x)J_{q'}(x)}{q'-q}\Big]
\end{aligned}
\tag{A10}
$$

 doi:10.20944/preprints202409.0474.v1

Appendix C. Example of Choosing q for σ_y

For the terms in the large braces of Equation 39, I start with $q = 1$ and choose the closest q' values that satisfy the even/odd rules.

$$\text{First sum choose } q' = -1, \quad \text{Second sum choose } q' = 2$$

$$\begin{aligned}&\left\{\frac{-J_1(x)J_2(x) - J_1(x)J_2(x)}{(-1)} + \frac{J_2(x)J_1(x) + J_2(x)J_1(x)}{(-2)}\right.\\ &\left.+\frac{-J_2(x)J_1(x) - J_2(x)J_1(x)}{(2)} + \frac{-J_1(x)J_2(x) - J_1(x)J_2(x)}{(1)}\right\}\end{aligned} \tag{A11}$$

$$= \frac{-4J_1(x)J_2(x)}{2} \rightarrow \frac{-4J_{q'-q}(x)J_{q'}(x)}{q'},$$

where the expression after the arrow can use whichever value of q'. For the next closest choices

$$\text{First sum choose } q' = 3, \quad \text{Second sum choose } q' = -2$$

$$\begin{aligned}&\left\{\frac{J_3(x)J_2(x) + J_3(x)J_2(x)}{(3)} + \frac{-J_2(x)J_3(x) - J_2(x)J_3(x)}{(2)}\right.\\ &+\frac{-J_2(x)(-1)J_3(x) - J_2(x)(-1)J_3(x)}{(-2)}\\ &\left.+\frac{-(-1)J_3(x)J_2(x) - (-1)J_3(x)J_2(x)}{(-3)}\right\}\end{aligned} \tag{A12}$$

$$= \frac{-4J_2(x)J_3(x)}{2} \rightarrow \frac{-4J_{q'-q}(x)J_{q'}(x)}{q'}.$$

Appendix D. Scattering Length

The nEDM experiment relies on UCN-^{3}He absorption which means their mutual interaction is of utmost importance. There will be a ^{3}He pseudomagnetic field present that only the neutrons will feel. Modulation of the dressing field will be used to offset this field. The scattering length for the neutron-^{3}He interaction is complex and can be decomposed into coherent and incoherent components. The scattering length is spin dependent and this is exploited in the nEDM experiment. The imaginary terms control the absorption rate and lead to the near zero cross section when the spins are parallel and large cross section when the spins are antiparallel. Whereas, the real terms give the Abragam pseudomagnetic field - the Fermi potential is spin dependent and mimics a magnetic field potential. As measured by Koester et al. [4], the coherent and incoherent scattering lengths are

$$b_c = 5.73 - 1.483i \quad \text{fm} \quad \text{and} \quad b_i = -2.5 + 2.568i \quad \text{fm}, \tag{A13}$$

giving

$$\begin{aligned}b_+ &= b_c + \sqrt{\frac{I}{I+1}}b_i = 4.29 + 0i \quad \text{fm}\\ b_- &= b_c - \sqrt{\frac{I}{I+1}}b_i = 10.07 - 5.93i \quad \text{fm};\end{aligned} \tag{A14}$$

where $+$ and $-$ refer to spins parallel and antiparallel respectively and I is nuclear spin. For neutrons and ^{3}He in the x-y plane, neutrons will precess about the helium spins and on average, the pseudo-

 doi:10.20944/preprints202409.0474.v1

magnetic field will remain in the x-y plane. This means the pseudomagnetic field is perpendicular to the electric field and reduces nEDM sensitivity.

Given the pseudomagnetic field is only seen by the neutrons, a deviation away from critical dressing is created as an extra field term will push the neutron effective Larmor frequency away from ^{3}He Larmor frequency. And although the pseudomagnetic field is quite small, about $1 \cdot 10^{-11}$T for the experiment's ^{3}He concentrations of $x_3 = 10^{-10}$ and near perfect polarization, it must be accounted for because of the high precision of the nEDM experiment. The pseudomagnetic field will be parallel to the ^{3}He spins and will have some average field value. In the lab frame on critical dressing, there were UCN and ^{3}He precessing about the z-axis while undergoing an oscillating precession about the x-axis. UCN will have a small additional precession about the ^{3}He and pick up a relative phase shift. Qualitatively, there would be separation that grows in time between the blue and red curves in Figure 4.4. The goal then is to offset this phase shift with dressing field modulations. The modulations will put the UCN and ^{3}He in front or behind one another and create a symmetry about critical dressing that offsets the asymmetric phase shift from the pseudomagnetic field. The following section will derive the theory for modulations and underscore the lack of dependence $< \sigma_x(t) >$ has on the pseudomagnetic field strength.

Appendix E. Third Order Correction to Eigenvalues Vanishing or Negelcted Terms

, the next terms would have $n' - n'' = \pm 1$ and some example values could be $n' = 2$ and $n'' = 1$. This means $n \neq 1, 2$ so that the smallest q and q′ available is for $n = 0$ or $n = 3$. Generally

$$\begin{aligned} &\frac{\overline{\langle n,m|}\sigma_z\overline{|n'',m''\rangle\langle n'',m''|}\sigma_z\overline{|n',m'\rangle\langle n',m'|}\sigma_z\overline{|n,m\rangle}}{(n-n')\omega(n-n'')\omega} \\ &= \frac{1}{8}\left[m''J_{-q'}(x)(-1)^{-q'} + mJ_{-q'}(x)\right]\left[m'J_{q''}(x)(-1)^{q''} + m''J_{q''}(x)\right] \\ &\times \frac{\left[mJ_q(x)(-1)^q + m'J_q(x)\right]}{(q\omega)(q'\omega)}. \end{aligned} \tag{A15}$$

The two cases above will yield the following terms

$$\begin{aligned} n' = 2, n'' = 1, n = 0 \\ q = 2, q' = 1, q'' = 1 \end{aligned}$$

$$\begin{aligned} &\frac{1}{8}\frac{\left[m''J_1(x) - mJ_1(x)\right]\left[-m'J_1(x) + m''J_1(x)\right]\left[mJ_2(x) + m'J_2(x)\right]}{(2\omega)(1\omega)} \\ &= \frac{mJ_1^2(x)J_2(x)}{2\omega^2} \end{aligned} \tag{A16}$$

$$\begin{aligned} n' = 2, n'' = 1, n = 3 \\ q = -1, q' = 2, q'' = 1 \end{aligned}$$

$$\begin{aligned} &\frac{1}{8}\frac{\left[m''J_2(x) + mJ_2(x)\right]\left[-m'J_1(x) + m''J_1(x)\right]\left[mJ_1(x) - m'J_1(x)\right]}{(-1\omega)(2\omega)} \\ &= -\frac{mJ_1^2(x)J_2(x)}{2\omega^2}, \end{aligned}$$

where certain conditions had to be chosen to avoid 0. In the first case: $m'' = -m', m' = m \rightarrow m'' = -m$. And for the second case: $m'' = -m', m' = -m \rightarrow m'' = m$. The two results in Equation 5.30 sum to 0. Many terms throughout this sum will cancel each other out. The ones that do not will be small enough relative to the $J_0(x)$ terms to only cause small errors as can be seen in plots below.

 doi:10.20944/preprints202409.0474.v1

References

1. Golub, R.; Lamoreaux, S.K. Neutron Electric-Dipole Moment, Ultracold Neutrons and Polarized ^{3}He. *Physics Reports* **1994**, *237*, 1–62.
2. Polonsky, N.; Cohen-Tannoudji, C. Interpretation Quantique de la Modulation de Frequence. *Le Journal de Physique* **1965**, *26*, 409–413.
3. Leung, K. The neutron electric dipole moment experiment at the Spallation Neutron Source. *EPJ Web of Conferences* **2019**, *219*.
4. Koester, L., H.R.; Seymann, H. *Nuclear Data Tables*, pp. 49–65.